

α —Calcitonin gene-related peptide inhibits autophagy and calpain systems and maintains the stability of neuromuscular junction in denervated muscles



Juliano Machado^{1,2,5,6}, Wilian A. Silveira^{1,8}, Dawit A. Gonçalves^{1,2,7}, Aline Zanatta Schavinski¹, Muzamil M. Khan^{3,4}, Neusa M. Zanon¹, Mauricio Berriel Diaz^{5,6}, Rüdiger Rudolf^{3,4}, Isis C. Kettelhut², Luiz C. Navegantes^{1,*}

ABSTRACT

Objective: Although it is well established that α -calcitonin gene-related peptide (CGRP) stabilizes muscle-type cholinergic receptors nicotinic subunits (AChR), the underlying mechanism by which this neuropeptide regulates muscle protein metabolism and neuromuscular junction (NMJ) morphology is unclear.

Methods: To elucidate the mechanisms how CGRP controls NMJ stability in denervated mice skeletal muscles, we carried out physiological, pharmacological, and molecular analyses of atrophic muscles induced by sciatic nerve transection.

Results: Here, we report that CGRP treatment *in vivo* abrogated the deleterious effects on NMJ upon denervation (DEN), an effect that was associated with suppression of skeletal muscle proteolysis, but not stimulation of protein synthesis. CGRP also blocked the DEN-induced increase in endocytic AChR vesicles and the elevation of autophagosomes per NMJ area. The treatment of denervated animals with rapamycin blocked the stimulatory effects of CGRP on mTORC1 and its inhibitory actions on autophagic flux and NMJ degeneration. Furthermore, CGRP inhibited the DEN-induced hyperactivation of Ca²⁺-dependent proteolysis, a degradative system that has been shown to destabilize NMJ. Consistently, calpain was found to be activated by cholinergic stimulation in myotubes leading to the dispersal of AChR clusters, an effect that was abolished by CGRP.

Conclusion: Taken together, these data suggest that the inhibitory effect of CGRP on autophagy and calpain may represent an important mechanism for the preservation of synapse morphology when degradative machinery is exacerbated upon denervation conditions.

© 2019 The Authors. Published by Elsevier GmbH. This is an open access article under the CC BY-NC-ND license (<http://creativecommons.org/licenses/by-nc-nd/4.0/>).

Keywords Autophagy; CGRP; Calpain; Neuromuscular junction; Skeletal muscle

1. INTRODUCTION

α -Calcitonin gene-related peptide (CGRP) is a 37-amino-acid neuropeptide that is well-known for exerting vasodilation and for controlling lipid and carbohydrate metabolism in adipose tissue, liver, and muscle [1–3]. CGRP is widely distributed in the central and peripheral nervous systems, including sensory and motor neurons [3]. Motor neurons release CGRP at the neuromuscular junction (NMJ) of skeletal muscle,

where it binds to CGRP receptors to induce both short and long-term actions mainly through cyclic adenosine monophosphate (cAMP)/protein kinase A (PKA)/cAMP response element binding protein (CREB) signaling pathway [3–6].

NMJ's are specialized chemical synapses between motor neurons and skeletal muscle fibers, and they mediate muscle contractions. Dysfunction of NMJ's leads to a variety of neuromuscular disorders, including congenital myasthenic syndromes (CMS) and myasthenia

¹Department of Physiology, Ribeirão Preto Medical School, University of São Paulo, Ribeirão Preto, São Paulo, Brazil ²Department of Biochemistry/Immunology, Ribeirão Preto Medical School/University of São Paulo, Ribeirão Preto, São Paulo, Brazil ³Institute of Molecular and Cell Biology, University of Applied Sciences Mannheim, Mannheim, Germany ⁴Institute of Medical Technology, University of Heidelberg and University of Applied Sciences Mannheim, Mannheim, Germany ⁵Institute for Diabetes and Cancer (IDC), Helmholtz Center Munich, 85764, Neuherberg, Germany ⁶Joint Heidelberg-IDC Translational Diabetes Program, Inner Medicine I, Heidelberg University Hospital, 69120, Heidelberg, Germany

⁷ Current address: School of Physical Education, Physiotherapy and Occupational Therapy, Federal University of Minas Gerais/UFMG, Exercise Physiology Laboratory, Belo Horizonte, Brazil.

⁸ Current address: Institute of Biological and Natural Science, Federal University of Triângulo Mineiro, Uberaba, Minas Gerais, Brazil.

*Corresponding author. Department of Physiology, Ribeirão Preto Medical School, University of São Paulo, Ribeirão Preto, SP, 14049-900, Brazil.

E-mails: juliano.machado@helmholtz-muenchen.de (J. Machado), silveira.wa@gmail.com (W.A. Silveira), dawit@ufmg.br (D.A. Gonçalves), alinezanatta@usp.br (A.Z. Schavinski), muzamil.m.khan@embl.de (M.M. Khan), neuzanon@yahoo.com.br (N.M. Zanon), mauricio.berrieldiaz@helmholtz-muenchen.de (M.B. Diaz), r.rudolf@hs-mannheim.de (R. Rudolf), idckette@fmrp.usp.br (I.C. Kettelhut), navegantes@fmrp.com.br, navegantes@fmrp.usp.br (L.C. Navegantes).

Received March 20, 2019 • Revision received June 23, 2019 • Accepted June 28, 2019 • Available online 3 July 2019

<https://doi.org/10.1016/j.molmet.2019.06.024>

gravis (MG) [7–9]. Loss of nerve-muscle communication caused by degeneration of motor neurons or motor neuron denervation (DEN) leads to increased turnover of nicotinic acetylcholine receptors (AChR) and muscle proteolysis [10–14]. Recently, it has been demonstrated that CGRP exerts trophic effects on the postsynaptic apparatus components in myotubes and mature muscles [15–17]. For example, application of CGRP increased the number and activity of AChR at the plasma membrane of primary myotubes *in vitro* [16,18]. Conversely, disruption of CGRP signaling accelerated the degeneration of NMJ and the loss of muscle performance induced by DEN [19]. However, the precise mechanisms by which CGRP maintains the metabolic stability of the AChR at NMJ as well as its regulatory effects on muscle protein metabolism under basal and muscle atrophy conditions have remained elusive.

Under catabolic conditions, the involvement of autophagy and calpains on the degradation of AChR and muscle proteolysis was found [13,20,21]. Autophagy is involved in the degradation of cytoplasmic targets, organelles, and plasma membrane proteins in a lysosome-dependent manner [21–24]. The activation of this system requires the induction of forkhead box O3 (FoxO3) transcription factor, which plays a critical role in muscle atrophy and is necessary and sufficient for the induction of autophagy in skeletal muscle *in vivo* and *in vitro* [11]. FoxO3 controls the transcription of autophagy-related genes, including microtubule-associated protein 1 light chain 3 beta (*Map1lc3b*), gamma-aminobutyric acid (GABA) A receptor-associated protein-like 1 (*Gabarap1*), and cathepsin L (*Ctsl*) [11,25]. In addition, muscle protein breakdown and autophagy may also be regulated by the mechanistic target of rapamycin complex 1 (mTORC1) pathway [26,27]. Although previous studies have shown that mTORC1 is required for regulation of NMJ homeostasis in *Drosophila* [28], in mammals such role on the NMJ remains unknown. Besides autophagy, also calpains play an important function on muscle protein metabolism and NMJ homeostasis [12,13,29,30]. Calpains are activated upon atrophic conditions, including muscle DEN [10,31,32] and in myasthenic models [12]. Furthermore, they may play a key role in the early steps of disassembly of sarcomeric proteins [29], impairment of neuromuscular transmission [12], and dispersion of AChR clusters at NMJ (Chen et al., 2007). The activation of the calpain system requires the elevation of intracellular Ca^{2+} levels [29] and consequent activation of calpain-1 and -2, the most abundant isoforms of the family of Ca^{2+} -dependent cysteine proteases. Upon DEN the elevation of cytosolic Ca^{2+} levels [33,34], NMJ degeneration [15,20] and muscle atrophy [10,11,34] are observed. Dispersion of AChR clusters at NMJs [12,13] and muscle protein degradation induced by calpains are inhibited by overexpression of its endogenous inhibitor calpastatin [12,13] as well as by cAMP agonists [35].

Although both the autophagic/lysosomal and the calpain systems are upregulated in several models of muscle atrophy [11,29,36], their regulation by extracellular signals is controversial and not fully understood. We and others [10,30,35,37] have demonstrated that cAMP-inducing agents, including catecholamines, beta-2 adrenergic agonists, and cAMP-phosphodiesterase inhibitors, inhibit these proteolytic processes. Similarly, also CGRP is capable of inducing cAMP production in muscle [38]. CGRP exerts a direct inhibitory action on autophagic-lysosomal proteolysis in extensor digitorum longus muscles (EDL) of denervated rats [38]. This suggests that CGRP might exert beneficial effects on NMJs upon DEN through its inhibitory action on autophagy and calpain systems, thus preserving the amount of AChR in the synapse of atrophic skeletal muscle. Here, we found that treatment with CGRP *in vivo* rescued the reduction of NMJ area in skeletal muscle of denervated mice, an effect that is apparently mediated through

mTORC1 and the suppression of autophagy. In addition, the present data show that the Ca^{2+} -dependent proteolytic system is also inhibited by CGRP, a mechanism that could also be important for the maintenance of the synapse.

2. MATERIALS AND METHODS

2.1. Animals, treatments and DEN surgery

For the majority *in vivo* experiments, sham-operated and 7-days-denervated, 12-wk-old C57/BL6 male mice, treated or not with CGRP (100 $\mu\text{g kg}^{-1}$; C0292 — Sigma—Aldrich) were used. Four-wk-old male Wistar rats, sham-operated and 7-days-denervated, treated or not with CGRP were also used for some *in vivo* experiments, in which the protein levels of the components from the Ca^{2+} -dependent proteolysis were measured. For *in vitro* experiments, isolated muscles incubated in the presence or absence of CGRP (10^{-6} M) from sham-operated and 7-days-denervated, 4-wk-old male Wistar rats were used. Subsequently, rates of proteolysis, proteolytic activities, protein synthesis, expression of mRNA and protein levels of the components from the Ca^{2+} -dependent proteolysis system, phosphorylation of the proteins from PKA/CREB signaling pathway, and intracellular levels of cAMP were measured in these samples. Young rats were used for *in vitro* experiments, because this procedure requires intact and sufficiently thin muscles to allow adequate diffusion of metabolites and oxygen [39]. Denervation was performed by dissecting out about 2 mm of the sciatic nerve roughly 1 cm above the popliteal fossa while the animals were under anesthesia (10 mg kg^{-1} ketamine and 85 mg kg^{-1} xylazine). DEN was chosen as an atrophy model because it induces a significant loss of contractile proteins and AChR degradation [10,23]. All animals were housed in a room with a 12-h light, 12-h dark cycle and were given free access to water and a normal laboratory chow diet. All experiments and protocols were in accordance with the ethical principles for animal experimentation adopted by the Brazilian College of Animal Experimentation and approved by Ribeirão Preto Medical School of the University of São Paulo—The Ethics Committee on Animal Use (CEUA 184/2010).

2.2. Evaluation of protein metabolism in rat isolated muscles

After euthanasia, isolated muscles used for determining *in vitro* protein synthesis or proteolysis were rapidly weighed, maintained at its resting length by holding their tendons in aluminum supports, and incubated at 37 °C in Krebs—Ringer bicarbonate buffer (pH 7.4, 5 mM glucose, equilibrated with 95% O_2 and 5% CO_2). Innervated and denervated muscles were incubated with either saline or CGRP. The concentration of CGRP for *in vitro* experiments was based on a dose—response curve of anti-proteolytic action of this peptide using rat isolated muscles [38].

2.3. Measurements of *in vitro* protein synthesis

Soleus muscles from normal and DEN rats were incubated in a Krebs—Ringer bicarbonate buffer that contained all amino acids at concentrations similar to those of rat plasma [40]. After a 1 h equilibration period, L-[U - ^{14}C]tyrosine (0.05 $\mu\text{Ci/ml}$) was added to the replacement medium and muscles were incubated for another 2 h. The rate of tyrosine incorporated into proteins using the specific activity of the intracellular pool of tyrosine of each muscle was calculated.

2.4. Measurements of *in vitro* overall proteolysis and proteolytic activities

After 2 h of incubation of rat *soleus* muscles in Krebs—Ringer bicarbonate buffer, the overall proteolysis and Ca^{2+} -dependent proteolytic activity were determined by measuring the rate of tyrosine release in

the incubation medium in the presence of cycloheximide (0.5 mM). Ca²⁺-dependent proteolysis was measured as described previously [10]. Tyrosine release was assayed using a fluorometric method [41].

2.5. Nonradioactive measurements of *in vivo* and *in vitro* protein synthesis with SUNSET

For *in vivo* measurements of protein synthesis, mice were treated with an intraperitoneal injection of 0.040 μmol g⁻¹ puromycin (P8833 — Sigma—Aldrich) dissolved in 100 μl of PBS. 30 min after injection, *gastrocnemius* muscles were extracted for western blot analysis (IV-SUNSET) of puromycin-labeled peptides. For *in vitro* measurements of protein synthesis, C2C12 myotubes were incubated for 30 min with media containing puromycin (1 μM). After 30 min of incubation with puromycin, the cells were extracted for the analysis of the amount of puromycin-labeled peptides by western blot.

2.6. *In vivo* electroporation of cDNA in mice skeletal muscle

Skeletal muscles were transfected by an optimized electroporation protocol based on the use of spatula electrodes to transfer cDNA *in vivo* into *tibialis anterior* (TA) muscle. peYFP-hLC3 (YFP-LC3) was kindly provided by Dr. M. Sandri (Venetian Institute of Molecular Medicine, Padua, Italy), pEGFP-N1 was obtained from Addgene Vector Database. Mice were anesthetized and a minor incision was performed on the hindlimb to expose the TA. This was injected with 30 μl of 0.9% saline containing 15 μg of purified plasmid DNA. Electric pulses were then applied using an electric pulse generator (CUY21; Tokiwa Science, Fukuoka, Japan) and two stainless steel spatula electrodes placed on each side of the isolated muscle. Four square-wave pulses with a pulse length of 20 ms and 200 ms intervals between each pulse were delivered at 21 V followed by four other pulses with the opposite polarity.

2.7. *In vivo* visualization of AChR puncta at NMJ and *in vivo* and *ex vivo* NMJ immunofluorescence

2.7.1. *In vivo* visualization of AChR puncta at NMJ

BGT-AlexaFluor647 (25 pmol, Life Technologies, B35450) was injected 24 h prior to microscopy into the TA to label surface exposed receptors, some of which are subsequently endocytosed. For *in vivo* visualization of AChR and NMJ area, green fluorescent BGT-AlexaFluor488 (25 pmol, Life Technologies, B13422) was injected 24 h prior to microscopy into the TA. The superficial 200 μm of TA were examined

in vivo with an upright Leica SP2 (Leica Microsystems) confocal microscope equipped with a 63 ×/1.2 NA water immersion objective. 3D stacks at 512 × 512-pixel resolution were taken [21]. Images were electronically processed using ImageJ/Fiji software (NIH). For quantitative analysis of vesicle numbers, the following procedure was used. The channel containing positive signals to BGT-AlexaFluor488 at NMJ was counted. This procedure yielded total amounts of AChR puncta per NMJ [21].

2.7.2. Whole muscles NMJ staining

Mouse *soleus* or TA muscles were rinsed in PBS and then fixed in 4% paraformaldehyde for 30 min [42]. Subsequently, the samples were rinsed for 3 × 10 min in PBS/glycine 0.1 M for 30 min and rinsed 3 × 10 min in PBS again. Then, the samples were quenched in ice cold 100% methanol for 5 min at -20 °C, rinsed for 3 × 10 min in PBS, and bathed in fluorescently conjugated BGT (diluted 1 : 200 in PBS) for 30 min. The muscles were mounted on slides with Dako fluorescent mounting medium and glass coverslips, sealed by clear nail polish on two sides. All imaging was performed on a Carl Zeiss LSM 7 MP Multiphoton Microscope using a 40 × objective. Maximum intensity projections of optical sections were created with ImageJ/Fiji software. The NMJ area labeled with BTX-488 was quantified using ImageJ, normalized for each experimental condition to the control.

2.8. Quantitative PCR

Total RNA was prepared from mouse TA muscles and C2C12 cells using TRIzol (Invitrogen®, Carlsbad, CA) kit. Complementary DNA was generated with Advantage ImProm-II reverse transcriptase (Promega®, Madison, WI). Real-time PCR was carried out using an ABI7500 sequence detection system (Applied Biosystems®, Foster City, CA). A SuperScript III Platinum SYBR Green One-Step RT-qPCR Kit with ROX (Invitrogen®) was used. The primers used are described in Table 1.

2.9. Western blot analysis

Muscle tissues (mouse *gastrocnemius* and rat *soleus*) and C2C12 cells were lysed and immunoblotted with anti-LC3 (1 : 1000; Cell Signaling 2775S); anti-calpain 1 large subunit detecting full-length calpain 1 as well as calpain 1 autoproteolytically cleaved at leucine 28 residue (1 : 750; Cell Signaling #2556S); anti-calpastatin (1 : 750; Cell Signaling #4146S); anti-phospho S6-(Ser235/236) (1 : 1000; Cell Signaling #2211S); anti-phospho-Ser256 FoxO1 (1 : 750; Cell Signaling #9461); phospho-Thr32 FoxO3 and phospho-Thr24 FoxO1

Table 1 — PCR primer sequences.

	Forward	Reverse
Rat <i>Capn2</i>	5' GAAGCCTCCCAATTTGTT 3'	5' CAGTGACGGAGTACGCATGTC 3'
Rat <i>Cast</i>	5'GCRATCACAGGACCTCTCCAGA 3'	5'GGTGAATCAGATGACAAGGCA3'
Mouse <i>Capn2</i>	5'GTTCTCTGCTGGCTGCTCTA 3'	5' CCTGATCGGATCAATTTCTG 3'
Mouse <i>Cast</i>	5'ATAGCTGCCCTCAACTACAGA 3'	5'TCTTTAGCCTTTGGCTTGGACA 3'
Mouse <i>Map1lc3b</i>	5' CGTCCTGGACAAGACCAAGT 3'	5' ATTGCTGTCCCGAATGTCTC 3'
Mouse <i>Gabarap1</i>	5'CATCGTGGAGAAGGCTCTCA3'	5' ATACAGCTGGCCCATGGTAG 3'
Mouse <i>ctsl</i>	5'GTGGACTGTTCTCACGCTTCAAG 3'	5' TCCGTCCTTCGCTCATAGG 3'
Mouse <i>Becn1</i>	5'GGCCAATAAGATGGGTCTGA 3'	5'CACTGCCTCCAGTGTCTTCA 3'
Mouse <i>Rpl39</i>	5' CAAAARCGCCCTATTCTCA 3'	5' AGACCCAGCTTCTCTCTCT 3'
Rat <i>Rpl39</i>	5' TCCTGGCAAAGAAACAAAAGC 3'	5' TAGACCCAGCTTCTCTCTCT 3'
Mouse <i>Chrn3</i>	5' CCAGAATGGCTCTTCTCTCAG 3'	5' GCTCTGCACCTTCTGG 3'
Mouse <i>Chrne</i>	5'GAGGGAGGCTATGTGAGCTG 3'	5'ACGGCAAAGATGAACCTCCAC 3'
Mouse <i>Chrna1</i>	5'TGCGGAAGGTTTTATCGAC 3'	5' CGGAGAGTGAAAGCCCATAG3'
Mouse <i>atrogen-1</i>	5'TGAACATCATGCAGAGGCTGA3'	5'GATCAAACGCTTGGCAATCTG3'
Mouse <i>Murf1</i>	5'ACCTGCTGGTGGAAACATC 3'	5'ACCTGCTGGTGGAAACATC 3'
Mouse <i>Tfeb</i>	5'CCACCCAGCCATCAACAC3'	5' CAGACAGATACTCCGAACCTT3'

(1 : 750; Cell Signaling #9464); FoxO1 (1 : 1000; Cell Signaling #9454); FoxO3 (1 : 1,000; Sigma—Aldrich AV38041); phospho-Thr37/46 4EBP1 (1 : 1,000; Cell Signaling #2855); 4EBP1 (1 : 1000; Cell Signaling #9452); phospho-Ser240/244 S6 (1 : 1000; Cell Signaling #2215); S6 (1 : 1000; Cell Signaling # #2217); anti- α -actinin (1 : 1000; Sigma—Aldrich A7811); anti-p35 (1 : 750; Santa Cruz Biotechnology sc-820); anti-Cdk5 (1 : 500; Santa Cruz Biotechnology sc-173); anti-endophilin-B1 (1 : 500; Santa Cruz Biotechnology sc-134843); anti- α -tubulin (1 : 1000; Santa Cruz Biotechnology sc-32293); anti- β -actin (1 : 1000; Santa Cruz Biotechnology sc-81178). Primary antibodies were detected using peroxidase-conjugated secondary antibodies (1 : 5000 for β -actin or α -tubulin and 1 : 1000 for the other primary antibodies) and visualized using ECL reagents by an ImageQuant 350 detection system (GE Healthcare, Piscataway, NJ). Band intensities were quantified using ImageJ (version 1.43u, National Institutes of Health, USA).

2.10. Determination of plasma insulin and muscle cAMP levels

Serum insulin levels and muscular cAMP levels were measured using a method based on a competitive enzyme immunoassay system (Millipore — EZRMI-13 k and GE Healthcare — RPN225, respectively).

2.10.1. Immunofluorescence on C2C12 myotubes and hela cells

To investigate the expression of AChR and the colocalization of calpain-1 with AChR, C2C12 myotubes cultured on poly-L-lysine (Sigma—Aldrich)-coated coverslips were fixed in 4% paraformaldehyde for 10–15 min. To study autophagic flux, HeLa cells (ATCC), were grown on coverslips and maintained in GM until 80–90% of confluency. Subsequently, the cells were transfected with YFP-LC3 vector using Lipofectamine™ 3000 (Thermo Fisher Scientific, Inc., Waltham, MA) according to the manufacturer's instructions. After 48 h of transfection, autophagy was induced by 2 h of incubation in starvation condition using Hank's Balanced Salt Solution (HBSS — GIBCO®). Because autophagy is a dynamic process with autophagosome synthesis, autophagosome fusion with the lysosome, and lysosomal degradation of autophagic substrates, the autophagic flux was analyzed in the presence of either, autophagolysosomal fusion inhibitors (chloroquine, 50 μ M; C6628 — Sigma—Aldrich; or bafilomycin A1, 100 nM; B1793 — Sigma—Aldrich), an mTOR inhibitor (rapamycin, 300 nM; R8781 — Sigma—Aldrich), or of CGRP. Then, cells were washed three times with PBS, permeabilised with 0.5% v/v Triton X-100 in PBS for 10 min and blocked with 5% w/v bovine serum albumin (BSA) in PBS for 45 min at room temperature. Coverslips were again washed three times with PBS and incubated overnight at 4 °C with anti-calpain 1 antibody (Santa Cruz Biotechnology; N-19; goat polyclonal; 1 : 100) in PBS containing 2% w/v BSA. Subsequently, cells were washed three times and followed by an incubation for 1 h with anti-goat IgG (1 : 200; Alexa Fluor 488-conjugated), DAPI (1 : 1000), and BGT-Alexa 647 (BTX-647; 1 : 200; Thermo Fisher Scientific). The fluorescence intensities of BGT, calpain-1 immunofluorescence, and YFP-LC3 puncta were assessed by confocal microscopy (Carl Zeiss LSM 7 MP Multiphoton Microscope using a 63 \times objective). BGT-488 or BGT-647 were quantified using ImageJ/Fiji as the intensity of the fluorescence signal minus background cytoplasmic fluorescence, normalized for each experimental condition to the control. Signals of AlexaFluor488-conjugated anti-goat IgG which stained calpain 1 was quantified using ImageJ/Fiji through automatic counting of the numbers of particles, normalized for each experimental condition to the control. The fluorescence intensity of BGT-Alexa Fluor 488/647 was quantified using ImageJ/Fiji, normalized for each experimental condition to the control.

2.10.2. Luciferase reporter assay

C2C12 cells were grown on in GM until 80–90% of confluency. Subsequently, cells were transfected with DBE-FoxO or MuRF1 luciferase and pRL-null-Renilla luciferase using Lipofectamine™ 3000 (ThermoFisher) according to the manufacturer's protocol. DBE-FoxO, MuRF1 Luciferase, and pRL-null-Renilla luciferase were kindly provided by Dr. M. Sandri (Venetian Institute of Molecular Medicine, Padua, Italy). Thereafter, GM medium was replaced with differentiation medium and experiments were performed after 3 days. C2C12 cells were homogenized in Passive Lysis Buffer using Tissue Lyzer (Qiagen), and luciferase activity was quantified using a Dual-Luciferase Reporter Assay (Promega). Foxo activity was determined by normalizing firefly luciferase activity (DBE-Foxo reporter) to pRL-null-Renilla luciferase activity.

2.11. Statistical analysis

Data were displayed as mean \pm standard error (SE). The statistical significance of differences was determined by one-way or two-way analysis of variance (ANOVA) followed by multiple comparison tests (Turkey's or Bonferroni's test). A significance level of 95% ($P < 0.05$) was accepted.

3. RESULTS

3.1. CGRP activates cAMP/PKA/CREB signaling pathway and abrogates the reduction of NMJ area

In agreement with the notion that CGRP exerts its physiological actions mainly through cAMP/PKA/CREB signaling pathway [4,17,38], we found that CGRP *in vitro* increased the cAMP levels as well as the phosphorylation levels of several PKA substrates, including CREB in both normal and DEN rat muscles (Figure 1A–F). cAMP levels increased rapidly within 15 min of CGRP in both control and denervated muscles but remained high until 120 min only in denervated muscles (Figure 1A,B). It is likely that the higher activity [43] and mRNA levels [44] of adenylyl cyclase accounts for the more-long lasting effect in cAMP levels induced by CGRP in denervated *soleus*. Under *in vivo* conditions, CGRP further increased the DEN-induced phosphorylation levels of PKA substrates and CREB (Figure 1G,H) in gastrocnemius of mice. Like in muscles, CGRP also activated PKA/CREB signaling in starved C2C12 myotubes (Figure 1I,J; DMEM low Glucose/Glucose 1 mM and without serum for 24 h). Since CGRP *in vitro* increased the amount of AChR at the plasma membrane [16], we evaluated chronic effects of *in vivo* treatment with CGRP with respect to the maintenance of NMJ area in denervated mice. CGRP treatment for 7 days prevented the reduction ($\sim 30\%$) of NMJ area in muscles of denervated mice (Figure 2A,B), but it did not abrogate the DEN-induced loss of muscle mass (Control: 0.523 ± 0.021 ; DEN: 0.214 ± 0.012 ; DEN + CGRP: 0.240 ± 0.019 mg.100 g BW⁻¹; n = 6–7). As previously described [45–47], we found that plasma levels of insulin were significantly decreased 1 h after a single injection of CGRP in mice (34.5 ± 8.9 vs 8.02 ± 0.9 μ UI/ml in controls). Acute treatment with CGRP at the first and fifth day of DEN partially rescued NMJ degeneration in denervated muscles (Figure 2C,D). Since CGRP did neither affect the incorporation of puromycin labeled peptides (Figure 2E,F) nor gene expression of *Chrna1*, *Chrne*, and *Chrng* (Figure 2G) in denervated rat muscles, the effects on NMJ area were likely not associated with alterations of general muscle protein synthesis or expression of AChR subunits. Also, CGRP did not increase the rates of protein synthesis as estimated by C¹⁴-tyrosine incorporation into total protein *in vitro* (Figure 2H). In contrast, CGRP (10^{-8} and 10^{-6} M) reduced the basal rates of tyrosine

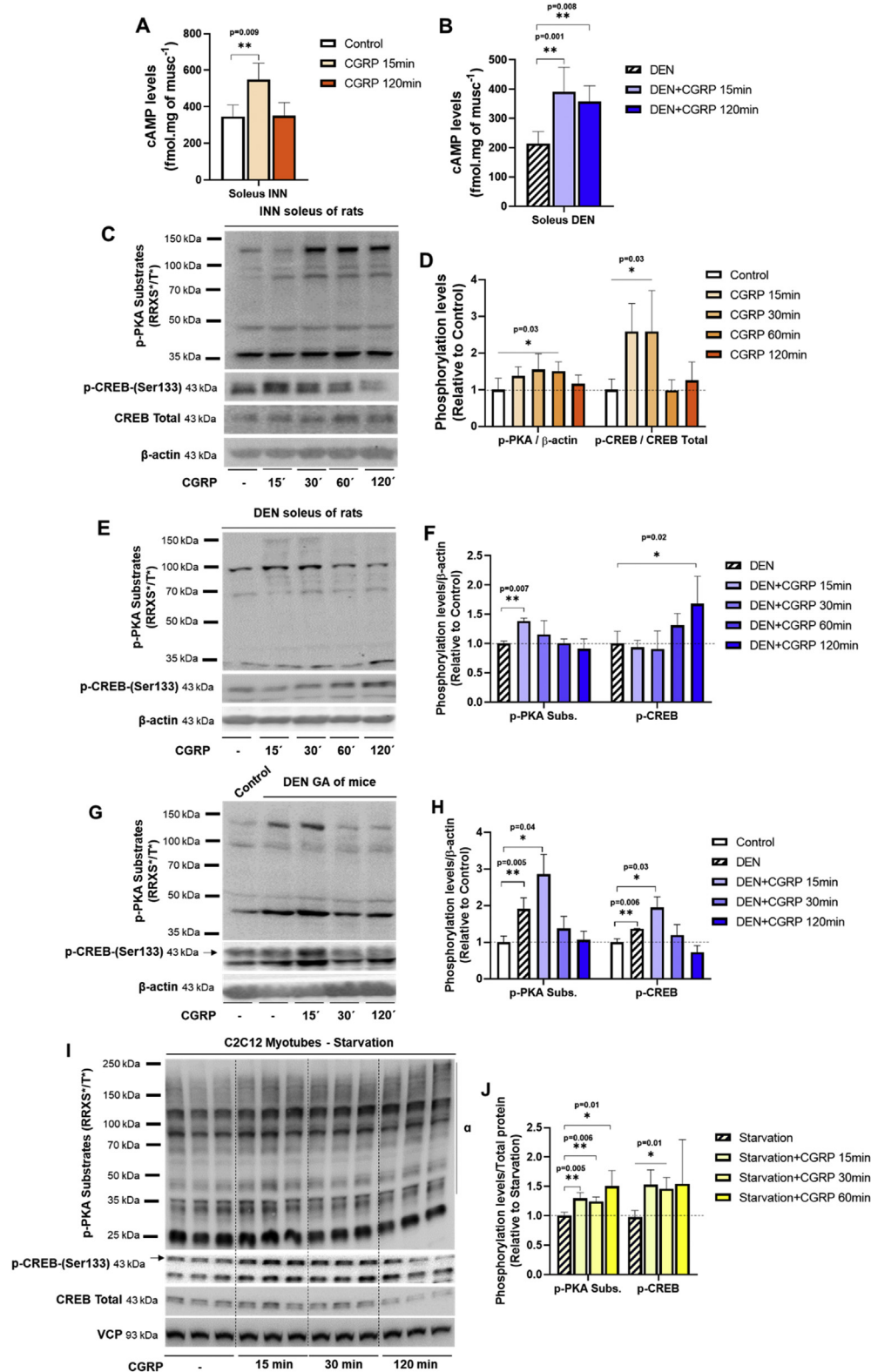


Figure 1: CGRP activates cAMP/PKA/CREB signaling pathway. (A) cAMP levels from *soleus* muscles incubated *in vitro* with CGRP (1 μ M) from control and (B) 7-days denervated rats. (C) Western blot and (D) densitometric analysis of phosphorylation levels of several substrates of PKA at Ser/Thr sites and CREB at Ser133 site in *soleus* muscles incubated *in vitro* with CGRP for 2 h from control rats. (E) Western blot and (F) densitometric analysis of phosphorylation levels of several substrates of PKA at Ser/Thr sites and CREB at Ser133 site in *soleus* muscles incubated *in vitro* with CGRP for 2 h from denervated rats. (G) Western blot and (H) densitometric analysis of phosphorylation levels of several substrates of PKA at Ser/Thr sites and CREB at Ser133 site in *gastrocnemius* muscles from denervated mice treated *in vivo* with a unique bolus of CGRP (100 μ g kg⁻¹). (I) Western blot and (J) densitometric analysis of phosphorylation levels of several substrates of PKA at Ser/Thr sites and CREB at Ser133 site in C2C12 myotubes under starvation (24 h of DMEM low glucose and without serum) condition and treated *in vitro* with CGRP for 2 h. Values are expressed as mean \pm SEM of 3–5 replicates per group.

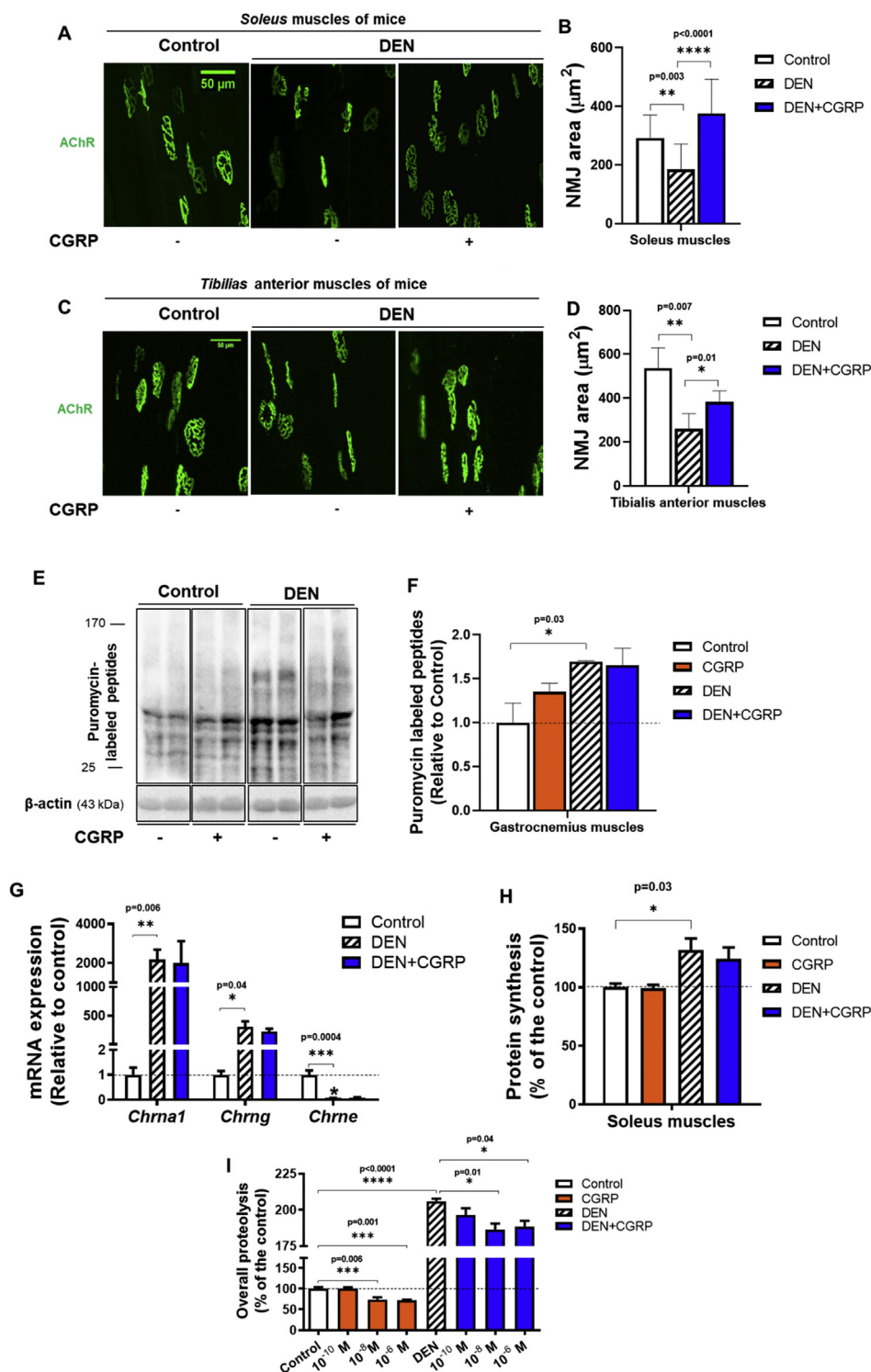


Figure 2: CGRP rescues the reduction of NMJ area in denervated muscles through a mechanism independent of protein synthesis. (A) AChR in whole *soleus* muscles from 7-days denervated mice daily treated or not with CGRP ($100 \mu\text{g kg}^{-1}$ for 7 days), labeled *ex vivo* with BGT-AlexaFluor488. Subsequently, confocal microscopy was performed and maximum z-projections of NMJs were obtained. (B) Quantitative analysis of NMJ area. Graph depicts the average of NMJ area of BGT-AF positive structures. (C) AChR in *tibialis* anterior muscles from denervated mice acutely treated or not with two injections of CGRP ($100 \mu\text{g kg}^{-1}$; at first and fifth day), labeled *in vivo* with BGT-AlexaFluor488. Subsequently, confocal microscopy was performed and maximum z-projections of NMJs were obtained. (D) Quantitative analysis of NMJ area. Graph depicts the average of NMJ area of BGT-AF positive structures. (E and F) *In vivo* effects of one single injection of CGRP ($100 \mu\text{g kg}^{-1}$; 2 h) on protein synthesis estimated by means of puromycin labeled peptides in *gastrocnemius* and on (G) mRNA levels of *Chna1*, *Chng*, and *Chre* subunits in *tibialis* anterior muscles of DEN mice. Gene expression was normalized to endogenous control, *Rpl39*, using the $\Delta\Delta\text{CT}$ method. (H) *In vitro* effects of CGRP ($1 \mu\text{M}$) on the rates of protein synthesis and on (I) overall proteolysis in isolated *soleus* muscles of rats. Data of protein synthesis and overall proteolysis are expressed as % of the values in control muscles considered as 100%, 0.214 ± 0.006 and $0.322 \pm 0.010 \text{ nmol mg}^{-1} \cdot 2 \text{ h}^{-1}$, respectively. Values are expressed as mean \pm SEM of 3–5 samples per group.

release by ~ 25% and attenuated the increase in protein breakdown induced by DEN (Figure 2I). In agreement with previous studies [48], DEN alone increased protein synthesis as estimated *in vivo* (Figure 2E,F) and *in vitro* (Figure 2H). Although the underlying mechanisms are still unknown this effect is likely important for increasing translation of the large number of mRNA species that are transcriptionally up-regulated following muscle inactivity [49]. These results suggest that an antiproteolytic action of CGRP, probably mediated by cAMP/PKA signaling, might be involved in the attenuation of AChR degradation and maintenance of NMJ upon DEN.

3.2. CGRP inhibits the formation of endo/lysosomal carriers containing AChR and autophagosomes at the NMJ and suppresses autophagy in mouse muscles

Previous studies have shown that DEN increases endocytic trafficking and degradation of AChR via autophagy in an endophilin-B1- and LC3-dependent manner [20,21], whilst lysosomal inhibitors decrease AChR degradation in mouse muscle cells [23]. Considering that CGRP inhibits protein degradation *in vitro* (Figure 2H) and hyperactivity of lysosomal proteolysis in rat denervated muscles [38], we assessed the *in vivo* role of CGRP in the modulation of endo/lysosomal carrier formation containing AChR at the NMJ. Mice were denervated and treated with a single injection of CGRP. After five days, a second injection of CGRP was administered, and after fourteen days the AChR were labeled with BGT-AlexaFluor647. On the following day, i.e. fifteen days after DEN, *in vivo* microscopy was performed. As shown in Figure 3, CGRP treatment blocked the increase (~3-fold) of the number of endocytic AChR-positive puncta per NMJ that was observed upon DEN (Figure 3A,B). In addition, CGRP treatment also blocked the elevation of LC3-positive autophagosomes per NMJ area in denervated muscles (Figure 3C,D). Previously, it was shown that CDK5 controls the activity of endophilin-B1, and its effects on autophagy in neural and muscle cells [21,50]. Endophilin-B1 is characterized by a N-BAR domain, necessary for phospholipid bilayer binding and curvature induction as well as a C-terminal SH3 domain, that allows interaction with proline-rich proteins, such as UVRAG (UV radiation resistance associated gene) protein [51]. In particular, binding of endophilin-B1 to UVRAG protein mediates Beclin1 recruitment to the phagophore and autophagy induction [51]. Here, we found that DEN increased the protein content of CDK5, endophilin-B1, and LC3II in mouse skeletal muscle by roughly 2 to 3-fold, an effect that was suppressed by CGRP (Figure 3E,F). Moreover, *in vivo* treatment with CGRP rescued the ~3 to 4-fold upregulation of the autophagy-related genes *Beclin-1* (*Becn1*), *Map1lc3b*, *Gabarapl1*, and *Ctsl* in denervated muscles (Figure 3G). Next, we examined the *in vitro* effects of CGRP on autophagy as induced by starvation in C2C12 cells. This revealed, that CGRP *in vitro* not only decreased the protein levels of LC3II and the ratio of LC3II/LC3I but also suppressed the expression of p62. This suggests that CGRP inhibits the autophagic flux and the autophagy machinery (Figure 3H,I). To further confirm the effects of CGRP on autophagic flux, we cultured C2C12 myotubes in the presence of HBSS, a serum and nutrient free medium that is well-known to induce autophagy *in vitro* [52]. For the measurement of autophagic flux, myotubes were kept in the absence or presence of Bafilomycin A1, an inhibitor of vacuolar H⁺-ATPase that prevents maturation of autophagic vacuoles by inhibiting fusion between autophagosomes and lysosomes [52]. As expected, the nutritional stress in C2C12 myotubes stimulated the autophagic flux and this effect was blocked by CGRP (Figure 3J). Consistently, CGRP also suppressed the ~2 to 6-fold induction of autophagic genes *Becn1*, *Map1lc3b*, and *Gabarapl1* in starved C2C12 myotubes (Figure 3K). Collectively, these data suggest that CGRP inhibits the endocytosis of

AChR at NMJs and the autophagic components involved in AChR degradation upon denervation.

3.3. CGRP inhibits the induction of FoxO family members and TFEB in mouse cell muscles

Because previous studies found that FoxO controls the expression of autophagy-related genes [11,53,54], we investigated the role of CGRP on the expression and activity of FoxO family members in mouse skeletal muscles upon atrophic conditions. In denervated mouse muscles, acute treatment with CGRP increased the phosphorylation levels of FoxO3a and FoxO1 (Figure 4A,B). Besides FoxO, the transcription factor EB (TFEB) is a newly discovered transcriptional factor and considered to act as a master regulator of autophagy and lysosomal biogenesis [55]. Here, we observed a DEN-induced elevation of *Tfeb* gene expression that was suppressed by *in vivo* treatment with CGRP (Figure 4C). Since the E3-ubiquitin ligase *MuRF1* is involved in the degradation of AChR at the NMJ [24] of atrophic muscles in an autophagy-dependent mechanism [20] and its expression is modulated by FoxO [54] and TFEB [56], we next tested the effects of CGRP on gene expression of *MuRF1*. Interestingly, the elevation of *MuRF1* induced by DEN was abrogated by *in vivo* treatment with CGRP (Figure 4D). Fittingly, CGRP *in vitro* increased the phosphorylation levels of several FoxO family members (Figure 4E,F) and blocked the upregulation of FoxO transcriptional activity (Figure 4G) that were induced by starvation in C2C12 cells. Furthermore, CGRP decreased the gene expression of *Tfeb* (Figure 4H) and *MuRF1* (Figure 4I) as well as *MuRF1* transcriptional activity (Figure 4J) under these conditions. Taken together, these data suggest that the transcriptional inhibition of autophagy-related genes and *MuRF1* mediated by FoxO and TFEB transcriptional factors are involved in the trophic effect of CGRP on NMJ in denervated muscles.

3.4. mTORC1 mediates the inhibitory effects of CGRP on autophagy and on the maintenance of NMJ in denervated muscles

Because mTORC1 inhibits autophagy [26,55] and is required for the regulation of NMJ homeostasis [28], we investigated whether mTORC1 could mediate the effects of CGRP on NMJ maintenance in denervated muscles. For this purpose, DEN mice were daily treated or not with CGRP for 7 days and/or rapamycin. Figure 5A,B show that the reduction of the NMJ area induced by DEN was rescued by daily treatment with CGRP, and this effect was blocked by co-treatment with rapamycin. To further demonstrate that CGRP indeed stimulates mTORC1 activity, DEN-mice were acutely treated with a single injection of CGRP and/or rapamycin. In agreement with previous studies [27], DEN alone increased the phosphorylation levels of S6, a downstream target of mTORC1 (Figure 5C,D). CGRP further enhanced the phosphorylation levels of S6 in denervated muscles and this effect was blocked by rapamycin treatment. In line with the hypothesis that mTORC1 mediates the effects of CGRP on autophagy, we observed that the downregulation on LC3II protein levels induced by the *in vivo* treatment with CGRP was blocked when the mice were cotreated with rapamycin (Figure 5E,F). In starved C2C12 cells, CGRP increased the phosphorylation levels of S6 (at Ser240 and 244, two specific residues of S6K1) and 4E-BP1 (Figure 5G,H). We next analyzed the autophagic flux in HeLa cells that were transiently transfected with YFP-LC3 and treated or not with CGRP, chloroquine, and rapamycin. Consistent with our previous observations, the increase in the number of YFP-LC3 puncta upon starvation was blocked by CGRP and this effect, in turn, was reverted by rapamycin (Figure 5I,J). Taken together, these data suggest that mTORC1 is required for the effects of CGRP on autophagy and the maintenance of NMJ in denervated muscles.

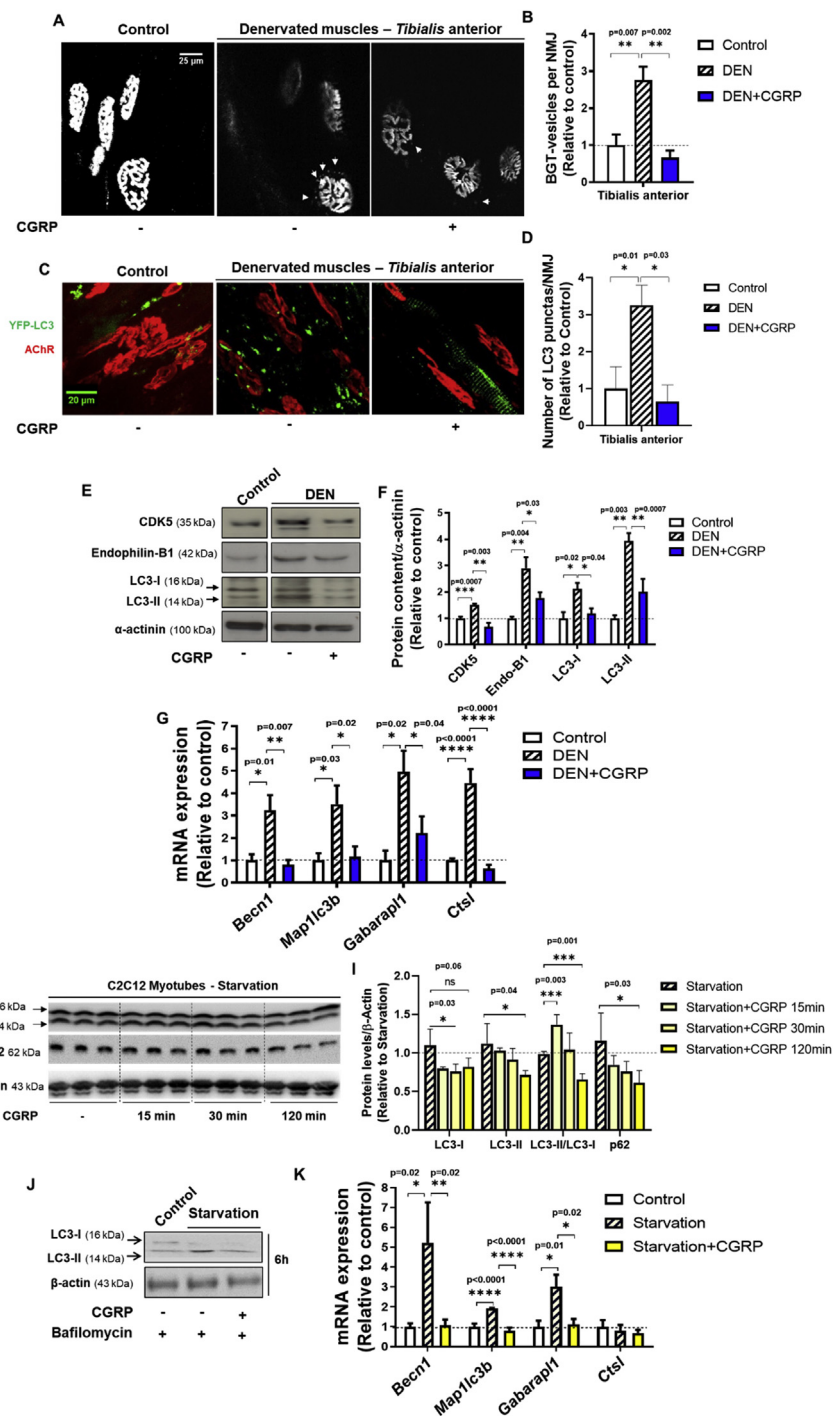


Figure 3: CGRP inhibits the endo/lysosomal carriers containing AChR at the NMJ as well as the autophagy in denervated muscles. (A) AChR in *tibialis* anterior muscles were labeled with BGT-AlexaFluor647 before *in vivo* microscopy analysis of the number of endo/lysosomal carriers containing AChR. Maximum z-projections of NMJs from control and DEN mice acutely treated with CGRP ($100 \mu\text{g kg}^{-1}$). Arrowheads indicate BGT-AF positive endo/lysosomal carriers. (B) Quantitative analysis of endo/lysosomal carriers. Graph depicts the average amount of BGT-positive vesicles per NMJ. (C) AChR in whole *tibialis* anterior muscles from 7-days denervated mice electroporated with YFP-LC3, daily treated or not with CGRP ($100 \mu\text{g kg}^{-1}$ for 7 days) was labeled *ex vivo* with BGT-AlexaFluor647. Subsequently, the confocal microscopy was performed and the maximum z-projections of NMJs were obtained and YFP-LC3⁺ puncta were automatically counted using Fiji software. (D) Numbers of YFP-LC3⁺ puncta per NMJ area. (E) Western blot and (F) densitometric analysis of Cdk5, endophilin-B1 and LC3 protein content normalized to α -actinin from *gastrocnemius* muscles of DEN mice treated with a single injection of CGRP. (G) RT-qPCR analysis of *Becl1*, *Map1lc3b*, *Gabarap1*, and *Ctst1* from *tibialis* anterior muscles of DEN mice treated with a single injection of CGRP. Gene expression was normalized to endogenous control, *Rpl39*, using the $\Delta\Delta\text{CT}$ method. (H) Western blot and (I) densitometric analysis of LC3 and p62 protein levels in C2C12 myotubes under starvation (24 h of DMEM low glucose and without serum) condition and treated *in vitro* with CGRP for 2 h. (J) Western blot analysis of LC3 in C2C12 myotubes incubated *in vitro* in starvation (HBSS for 6 h) condition with CGRP ($1 \mu\text{M}$) in the presence of bafilomycin A1 (100 nM). (K) RT-qPCR analysis of *Becl1*, *Map1lc3b*, *Gabarap1*, and *Ctst1* from C2C12 myotubes incubated *in vitro* in HBSS for 3 h with CGRP. Gene expression was normalized to endogenous control, *Rpl39*, using the $\Delta\Delta\text{CT}$ method. In the quantitative analysis, values are expressed as mean \pm SEM of 3–5 replicates per group.

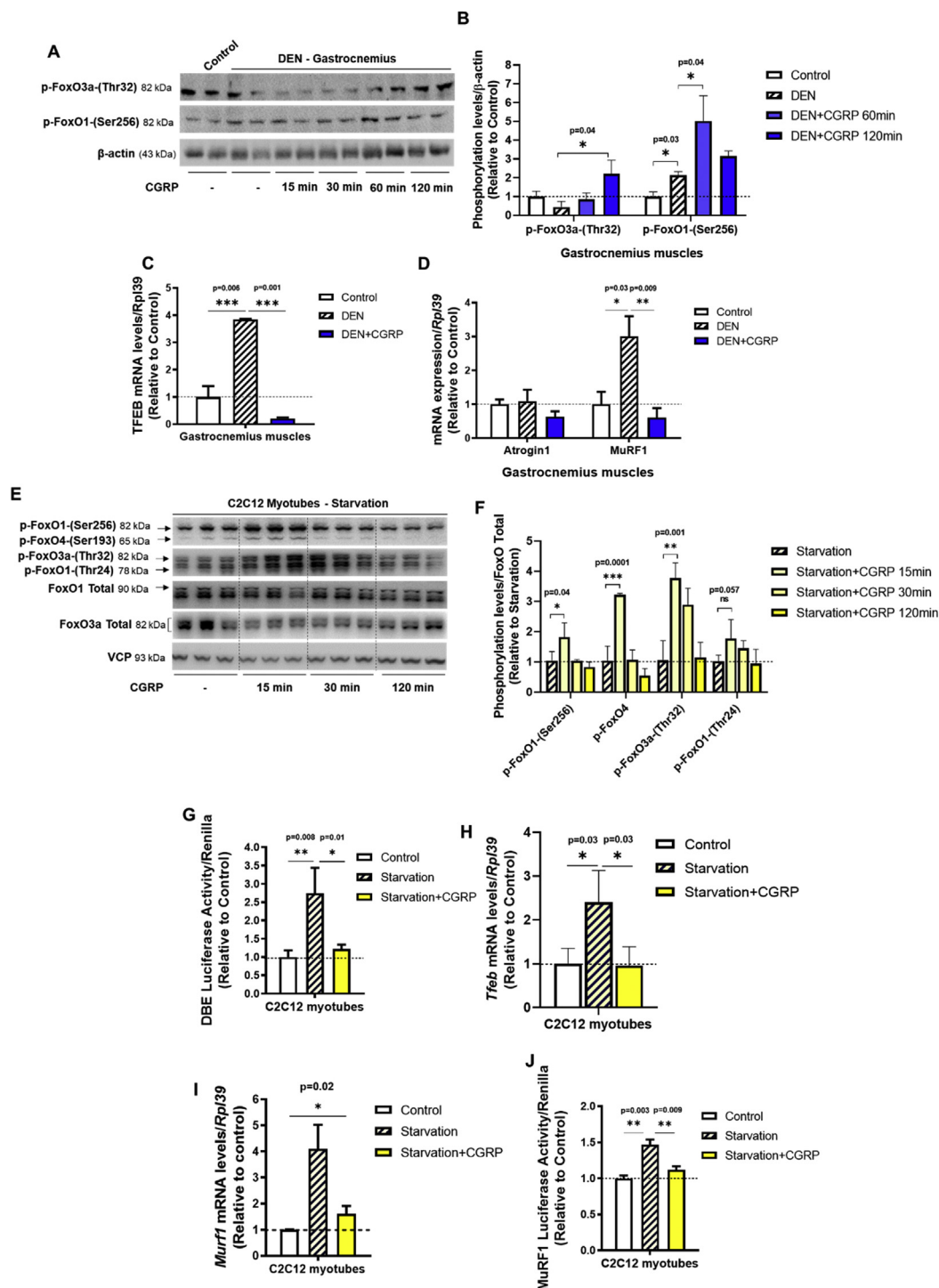


Figure 4: CGRP inhibits the induction of FoxO family members and TFEB in mouse cell muscles induced by atrophic conditions. (A) Western blot and (B) densitometric analysis of FoxO1-(Ser256) and FoxO3-(Thr32) phosphorylation levels normalized to β -actin from *gastrocnemius* muscles of 7-days denervated mice treated with a single injection of CGRP ($100 \mu\text{g kg}^{-1}$). RT-qPCR analysis of (C) TFEB, (D) atrogin1 and MuRF1 from tibialis anterior muscles of DEN mice treated with a single injection of CGRP. Gene expression was normalized to endogenous control, Rpl39, using the $\Delta\Delta\text{CT}$ method. (E) Western blot and (F) densitometric analysis of phosphorylation levels of several FoxO family members in C2C12 myotubes under starvation (24 h of DMEM low glucose and without serum) condition and treated *in vitro* with CGRP for 2 h. (G) FoxO transcriptional activity of C2C12 myotubes incubated in HBSS medium in the presence or absence of CGRP ($1 \mu\text{M}$; 2 h). Firefly/renilla luciferase activity was measured as described in the materials and methods. RT-qPCR analysis of (H) Tfeb and (I) MuRF1 from C2C12 myotubes incubated *in vitro* in HBSS for 3 h with CGRP. Gene expression was normalized to endogenous control, Rpl39, using the $\Delta\Delta\text{CT}$ method. (J) MuRF1 transcriptional activity of C2C12 myotubes incubated in HBSS medium in the presence or absence of CGRP ($1 \mu\text{M}$; 2 h). Firefly/renilla luciferase activity was measured as described in the materials and methods. Values are expressed as mean \pm SEM of 3–5 replicates per group. (I) MuRF1 from C2C12 myotubes incubated *in vitro* in HBSS for 3 h with CGRP. Gene expression was normalized to endogenous control, Rpl39, using the $\Delta\Delta\text{CT}$ method. (J) MuRF1 transcriptional activity of C2C12 myotubes incubated in HBSS medium in the presence or absence of CGRP ($1 \mu\text{M}$; 2 h). Firefly/renilla luciferase activity was measured as described in the materials and methods. Values are expressed as mean \pm SEM of 3–5 replicates per group.

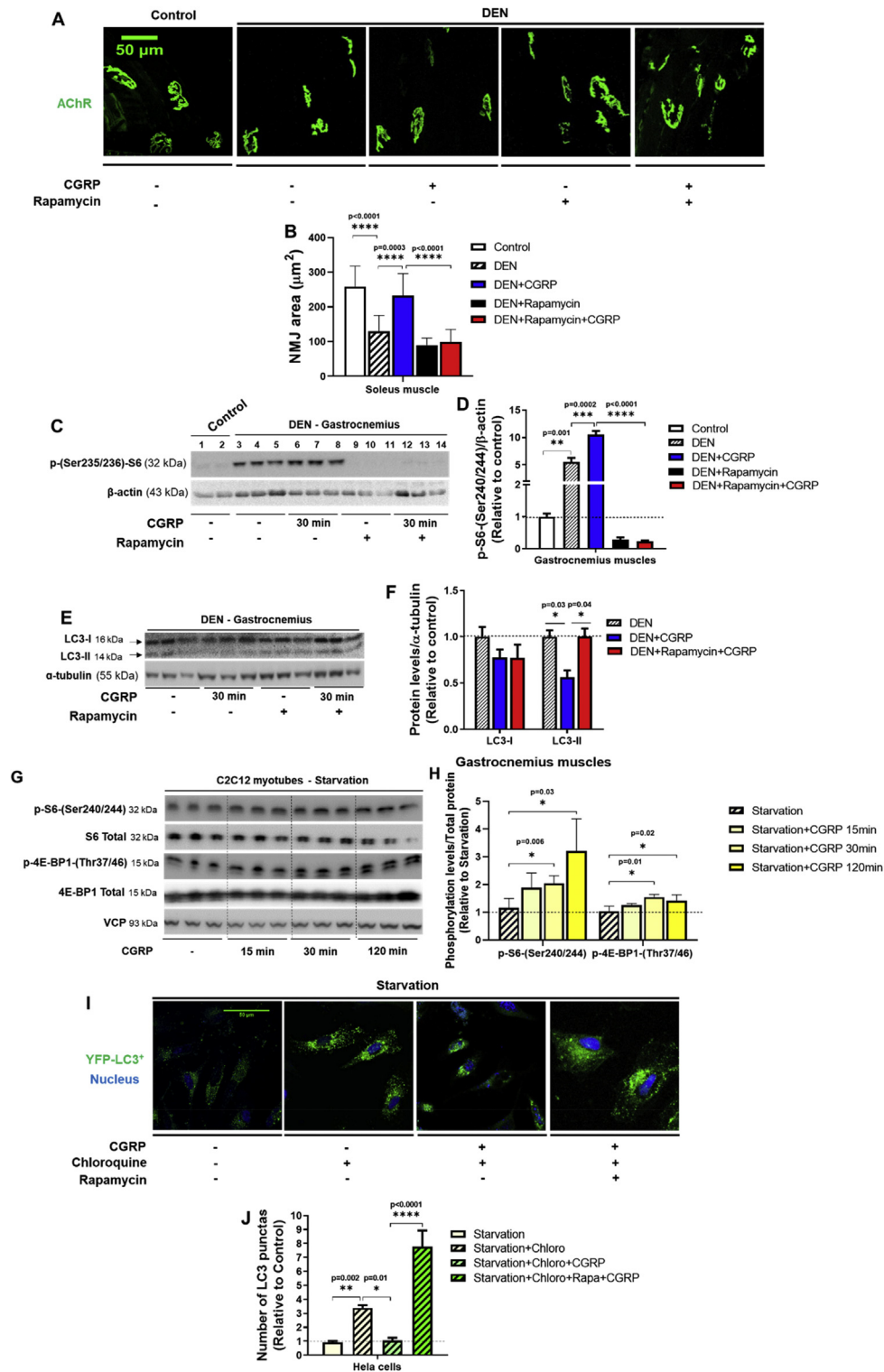


Figure 5: The mTORC1 signaling pathway is induced by CGRP and mediates its effects in NMJ area maintenance and autophagy in mice skeletal muscles. (A) AChR in whole *soleus* muscles from 7-days denervated mice daily treated or not with CGRP ($100 \mu\text{g kg}^{-1}$ for 7 days) and rapamycin (1.5 mg kg^{-1} for 7 days) was labeled *ex vivo* with BGT-AlexaFluor488. Subsequently, the confocal microscopy was performed and the maximum z-projections of NMJs were obtained. **(B)** Quantitative analysis of NMJ area. **(C)** Western blot and **(D)** quantitative analysis of S6-(Ser235/236) phosphorylation levels normalized to β -actin in *gastrocnemius* muscles from denervated mice treated with a single injection of rapamycin (1.5 mg kg^{-1}) and/or CGRP ($100 \mu\text{g kg}^{-1}$). **(E)** Western blot and **(F)** quantitative analysis of LC3 protein levels normalized to α -tubulin in *gastrocnemius* muscles from denervated mice treated with a single injection of rapamycin (1.5 mg kg^{-1}) and/or CGRP ($100 \mu\text{g kg}^{-1}$). **(G)** Western blot and **(H)** densitometric analysis of phosphorylation levels of S6 at Ser240/244 and 4E-BP1 at Thr37/46 sites in C2C12 myotubes under starvation (24 h of DMEM low glucose and without serum) condition and treated *in vitro* with CGRP for 2 h. **(I)** HeLa cells were transfected with YFP-LC3 and after 48 h the cells were incubated *in vitro* in HBSS medium and treated with chloroquine (50 μM), rapamycin (300 nM), and CGRP (1 μM ; 3 h). **(J)** Numbers of YFP-LC3⁺ puncta per HeLa cell. Values are expressed as mean \pm SEM of 3–5 replicates per group.

3.5. CGRP inhibits the Ca^{2+} -dependent proteolytic system in denervated skeletal muscles

Considering that calpains are activated upon denervation [10,31,32], impair neuromuscular transmission [12], and are regulated by cAMP/PKA signaling, we evaluated whether CGRP could modulate the activity of the Ca^{2+} -dependent proteolytic system in rodent skeletal muscles. As shown in Figure 6A,B, a single injection of CGRP in denervated mice significantly inhibited the calpain activity as indicated by elevated protein content of autolyzed calpain-1 and p25, the latter being the cleavage form of the calpain substrate protein p35. DEN increased

gene expression of *calpain-2* (*Capn2*) and reduced the mRNA levels of *calpastatin* (*Cast*), the endogenous inhibitor of calpains, whilst the acute treatment with CGRP abolished such effects (Figure 6C). Furthermore, in rat muscles *in vitro*, the addition of CGRP to the incubation medium reduced Ca^{2+} -dependent proteolysis in both control and denervated muscles by about 20–25% (Figure 6D). Next, we assessed the role of chronic treatment with CGRP (i.e., for 7 days) in the calpain system in rat muscles. Although chronic treatment with CGRP did not alter calpastatin levels, the protein content of autolyzed calpain-1 was significantly decreased by CGRP (Figure 6E,F). Taken

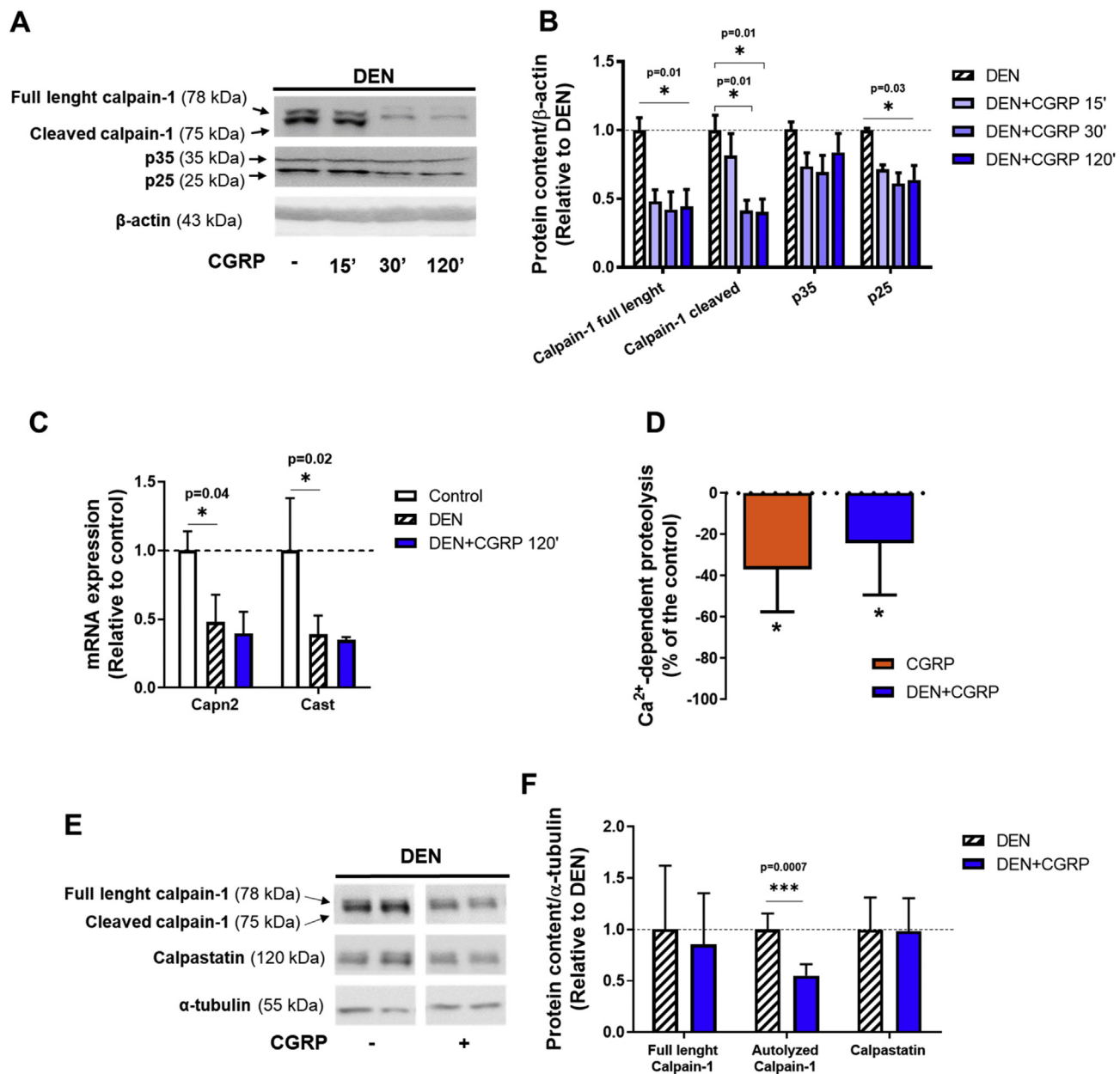


Figure 6: CGRP inhibits the Ca^{2+} -dependent proteolysis and the calpain activity in denervated muscles. (A) Western blot and (B) densitometric analysis of p35, p25, and calpain-1 protein content normalized to β -actin from *gastrocnemius* muscles of denervated mice treated with a single injection of CGRP ($100 \mu\text{g kg}^{-1}$; 2 h). (C) RT-qPCR analysis of *Capn2* and *Cast* of *tibialis* anterior muscles from denervated mice 2 h after a single injection of CGRP. Gene expression was normalized to endogenous control, *Rpl39*, using the $\Delta\Delta\text{CT}$ method. (D) *In vitro* effects of CGRP ($1 \mu\text{M}$) on Ca^{2+} -dependent proteolytic activity in control and denervated *soleus* muscles of rats. Data of Ca^{2+} -dependent proteolytic activity are expressed as % of the values of the control and denervated muscles considered as 100%, 0.122 ± 0.012 and $0.131 \pm 0.007 \text{ nmol of Tyr mg}^{-1} 2 \text{ h}^{-1}$, respectively. (E) Western blot and (F) densitometric analysis of calpain-1, and calpastatin protein content normalized to α -tubulin in skeletal muscles from control and denervated *soleus* muscles of rats chronically treated with CGRP ($100 \mu\text{g kg}^{-1}$ for 7 days). Values are expressed as mean \pm SEM of 3–5 replicates per group.

together, these data show that CGRP directly inhibits the basal and denervation-induced calpain activation in skeletal muscle from rodents.

3.6. CGRP suppresses the activation of calpain in muscle cells and in parallel stabilizes AChR at plasma membrane

Because cholinergic stimulation causes calpain activation and dispersal of AChR clusters [13], we investigated the *in vitro* effect of CGRP on calpain activity and amount of AChR in muscle cells incubated with carbachol (CCh), a nonhydrolyzable cholinergic agonist. As shown in Figure 7A, CCh increased the Ca^{2+} -dependent proteolysis in isolated rat muscles *in vitro* by about 2.5-fold. This effect was attenuated (~30%) by CGRP (Figure 7A). Moreover, CGRP blocked the ~6-fold increase in autolysis of calpain-1 that was induced by CCh in C2C12 myotubes (Figure 7B,C). To investigate whether CGRP maintains the stability of AChR at the plasma membrane by a mechanism independent of protein synthesis, C2C12 myotubes were incubated with CCh and/or CGRP in the presence of cycloheximide (CHX), a protein synthesis inhibitor. Subsequently, cells were fixed and AChR were labeled with BGT-AlexaFluor488. As shown in Figure 7D–G, CGRP treatment rescued the decreased expression of AChR in C2C12 myotubes upon CCh when protein synthesis was inhibited by CHX. As expected, the decreased expression of AChR and the increased number of calpain-1 positive structures (Figure 7H,I) induced by CCh were both blocked by CGRP in C2C12 myotubes. Importantly, *in vivo* treatment with calpeptin, a well-known cell-permeable calpain inhibitor for 7 days mimicked the effects of CGRP, and partially reverted the reduction of NMJ sizes induced by DEN (Figure 7J,K). Taken together, these results show that CGRP suppresses the activation of calpain and autophagy in muscle cells and in parallel stabilizes AChR at the plasma membrane.

4. DISCUSSION

The present data show that treatment with CGRP *in vivo* rescued the reduction of NMJ area in skeletal muscle of denervated mice. This effect was associated with suppression of a DEN-induced elevation of the number of endocytic/lysosomal carriers containing AChR at the synapse. Likely, this trophic effect of CGRP at the NMJ was due to reduced AChR degradation, since CGRP *in vitro* increased AChR content in myotubes even in the presence of CHX, a condition that blocks protein synthesis. Moreover, CGRP inhibited overall proteolysis in normal and denervated muscles but did not affect the rate of protein synthesis. Along these lines, it has been consistently shown that lysosomal inhibitors reduce the degradation of AChR in muscle cells demonstrating an important role of this pathway for the regulation of AChR abundance [23]. In a previous study, we have demonstrated that CGRP inhibits lysosomal proteolysis in glycolytic skeletal muscles of rats [38]. In extension to this concept, we now present strong evidence that CGRP suppressed the autophagic flux in denervated oxidative and glycolytic mouse muscles as well as in starved C2C12 myotubes. We found that upon muscle DEN, CGRP treatment blocked the elevation of well-known markers of endocytic/lysosomal carriers involved in the AChR degradation, including Cdk5, endophilin-B1, and LC3II. These data are consistent with the findings that the deletion of $Cdk5^{-/-}$ in primary myotubes increases AChR clusters [57] and that muscle DEN increases the activity of endophilin-B1, a substrate of Cdk5, as well as the degradation of AChR at NMJ through the autophagic-lysosomal system [21]. In fact, the number of vesicles positive for AChR as well as their colocalization with endophilin-B1 were increased upon DEN [21]. Also, we observed that CGRP treatment inhibited the

upregulation of *Becn1*, *Map1lc3b*, *Gabarapl1*, and *Ctstl* mRNA levels in either denervated muscles or C2C12 myotubes, indicating that CGRP suppresses the autophagic-lysosomal system, at least in part, by transcriptional mechanisms. Although it cannot be ruled out that these effects might also be due to CGRP-induced changes in mRNA degradation rates of such genes, the present study clearly shows that CGRP inhibits FoxO activity, which is the main transcriptional factor involved in the control of the autophagic-lysosomal system. Previous studies have shown that under atrophic conditions such as muscle DEN or starvation, the transcriptional activity of FoxO is increased and that FoxO activates several autophagy-related genes including *Becn1*, *Map1lc3b*, *Gabarapl1*, and *Ctstl* [11,53]. In addition, our findings show that CGRP increases the gene expression of TFEB, a transcriptional factor that not only controls the expression of autophagy-related genes [11,53], but also the expression of genes involved in lysosomal biogenesis [55]. Interestingly, FoxO [54] and TFEB [56] are involved in the control of MuRF1 gene expression, an E3-ligase involved in autophagy-mediated degradation of AChR [20] upon atrophic conditions [24]. In agreement with these findings, we observed that CGRP inhibited DEN-induced upregulation of MuRF1 suggesting that the suppression of this E3-ligase could be an additional mechanism by which CGRP stabilizes AChR at NMJ. Despite these inhibitory effects on MuRF1, CGRP does not modulate the proteolytic activity of the ubiquitin-proteasome system [38]. Since it is well established that loss of innervation causes muscle wasting by the induction of the proteasomal system [58,59], this could explain why CGRP treatment did not rescue the denervation-induced loss of muscle mass.

Previously, we demonstrated that CGRP exerted its inhibitory actions on FoxO activity through PKA and not AKT [38]. PKA is well known to be involved in the physiological effects of this peptide [3,4,17]. Because mTORC1 can be stimulated by both AKT and PKA [60,61] and negatively controls autophagy [26,55], we investigated whether mTORC1 might be involved in the suppressive effects of CGRP on autophagy and on NMJ maintenance. Although several studies have shown that mTORC1 exerts an important role on synaptic plasticity in rodent central nervous system [62–66], to our knowledge there is only one study reporting a role of TORC1 in the maintenance and activity-dependent homeostatic response in NMJ of *Drosophila* [28]. Here, we show that CGRP, like other cAMP-stimulating signals [61], activates mTORC1 signaling in starved C2C12 myotubes and in denervated muscles. Furthermore, rapamycin abolished the effects of CGRP on mTORC1 signaling and autophagy. It is noteworthy that rapamycin also blocked the suppression of autophagosome formation by CGRP as well as the trophic effect of this peptide on the maintenance of NMJ area in denervated muscles. Importantly, mTORC1 is known as the main negative regulator of TFEB activity, autophagy, and lysosomal proteolysis [55,67], and the lysosome is the main organelle involved in the degradation of AChR [23]. Because CGRP was found to control AChR abundance at the plasma membrane of differentiated myotubes independent of protein synthesis [16], our current and previous data [38] suggest that the ability of CGRP to prevent NMJ degeneration in the setting of DEN is due to the activation of mTORC1, leading to reduced autophagy and AChR degradation. The fact that CGRP activates mTORC1 but does not stimulate protein synthesis is consistent with recent studies, which demonstrated that mTORC1 can inhibit autophagy independent of the control of protein synthesis [68,69]. Mechanistically, the full activity of mTORC1 depends on its lysosomal localization mediated by the Regulator-Rag complex [70,71] followed by its interaction with Rheb [71], a key activator of mTORC1 stimulated by insulin [69]. Therefore, the absence of protein synthesis-inducing effects of CGRP here reported could be explained, at least in part, by

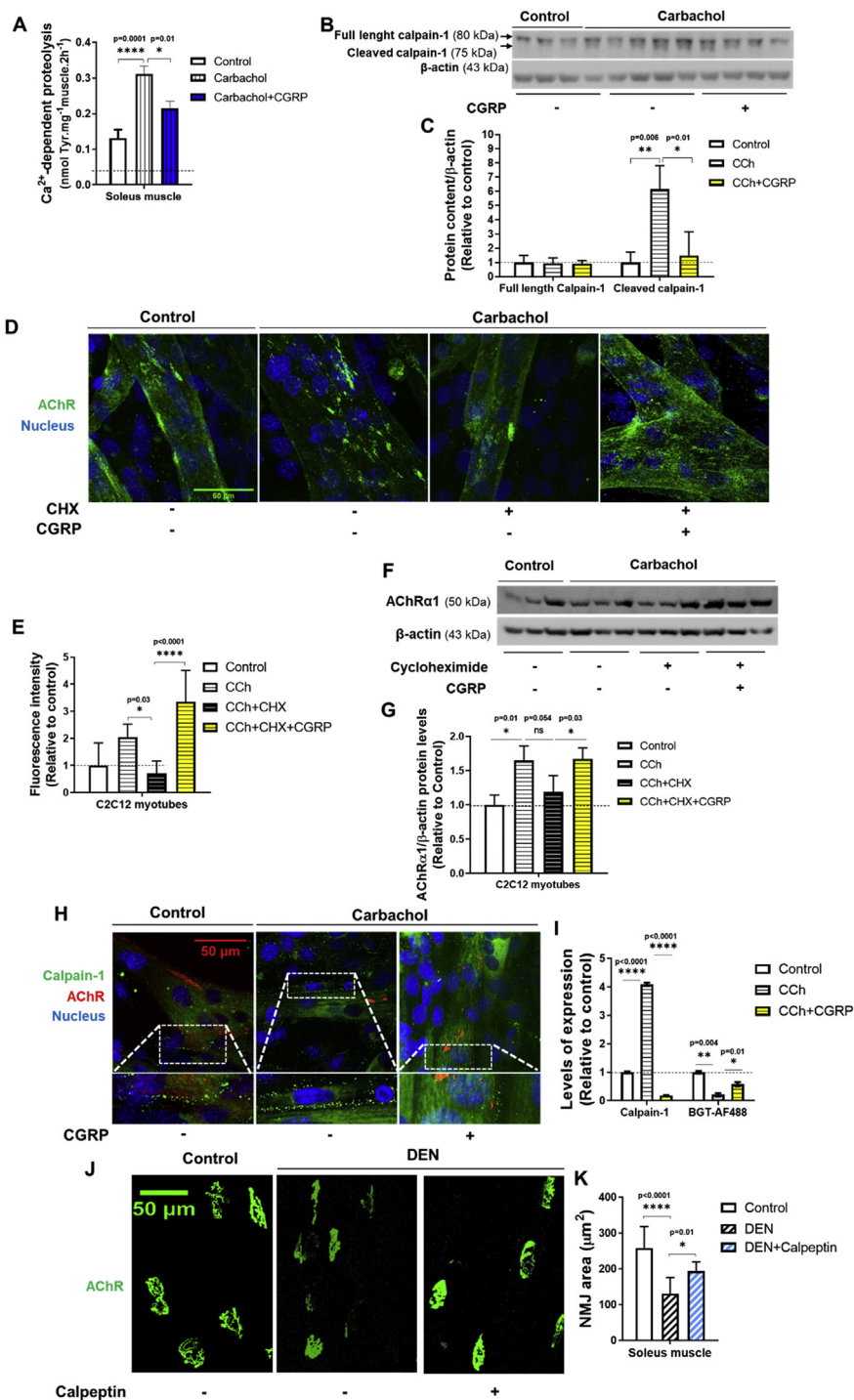


Figure 7: CGRP inhibits the calpains and preserve the amount of AChR at the plasma membrane in muscle cells. (A) *In vitro* effects of CGRP (1 μM) on carbachol (100 μM)-induced activation of Ca^{2+} -dependent proteolysis in rat *soleus* muscles. (B) Western blot and (C) densitometric analysis of the calpain-1 autolysis induced by carbachol (100 μM) and $CaCl_2$ (1 mM) in C2C12 myotubes, in the presence or absence of CGRP (1 μM; 3 h). (D) Immunofluorescence and (E) fluorescence intensity of AChR labeled with BGT-AlexaFluor488 in C2C12 myotubes treated with carbachol (100 μM) and $CaCl_2$ (1 mM) in the presence or absence of cycloheximide (500 μM) and/or CGRP (1 μM; 3 h). *In vitro* microscopy was performed, and fluorescence intensity was determined using ImageJ (Fiji). Maximum z-projections of confocal stacks showing automatically segmented of AChR in C2C12 myotubes. The receptors and nucleus signals in the overlay panels are shown in green and blue, respectively. (F) Western blot and (G) densitometric analysis of AChR in C2C12 myotubes treated with carbachol (100 μM) and $CaCl_2$ (1 mM) in the presence or absence of cycloheximide (500 μM) and/or CGRP (1 μM; 3 h). (H and I) Immunofluorescence and quantification of AChR and calpain-1 expression in C2C12 myotubes treated with carbachol (100 μM) and $CaCl_2$ (1 mM), in the presence or absence of CGRP (1 μM; 3 h). *In vitro* microscopy was performed, and fluorescence intensity was determined using ImageJ (Fiji). Maximum z-projections of confocal stacks showing automatically segmented of AChR in C2C12 myotubes. The AChR labeled with BGT-AlexaFluor647 (far red), calpain labeled with AF488 (green), and nucleus labeled with DAPI (blue) signals in the overlay panels. (J) Immunofluorescence and (K) average of NMJ area from AChR labeled *ex vivo* with BGT-AlexaFluor488 in whole *soleus* muscles from 7-days denervated mice daily treated or not with calpeptin (15 mg kg⁻¹ for 7 days). The results from control and DEN group are the same used in Figure 5A. Subsequently, the confocal microscopy was performed and the maximum z-projections of NMJs were obtained. Values are expressed as mean ± SEM of 3–5 replicates per group.

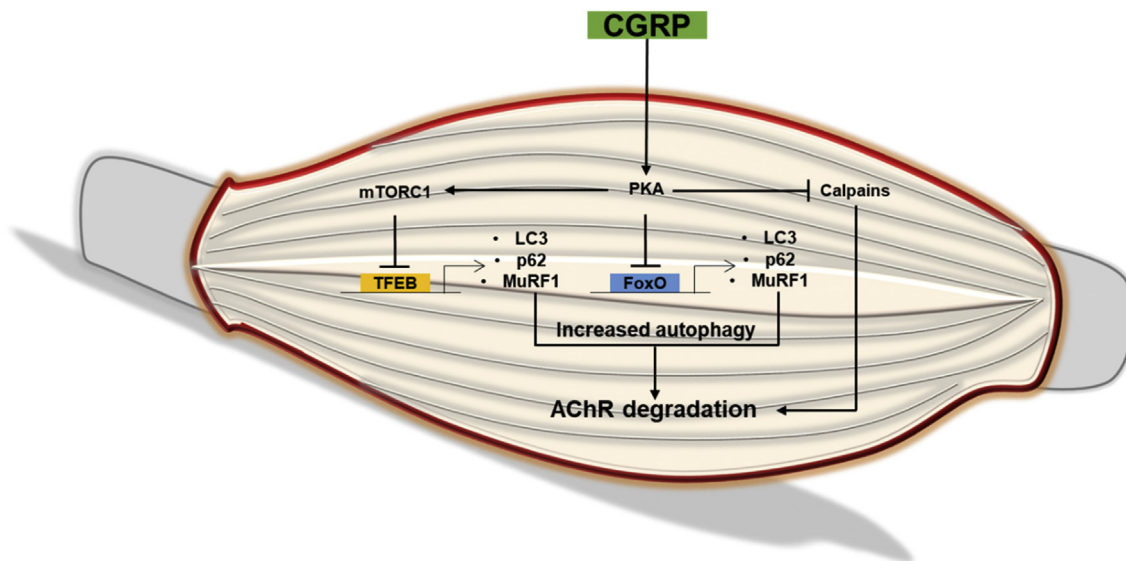


Figure 8: Hypothesis of how CGRP maintains the stability of AChR and suppresses autophagy and calpain systems in denervated skeletal muscle. 1. CGRP inhibits the transcriptional activity of FoxO and TFEB. FoxO is a well-known transcriptional factor involved in the control of LC3 and autophagy [1]. 2. TFEB is a transcriptional factor master regulator of autophagosome and lysosome biogenesis [2]. 3. Furthermore, mTOR is a direct negative regulator of TFEB activity [2]. 4. Both FoxO3 [3] and TFEB [4] control the gene expression of E3 ubiquitin ligase MuRF1 upon atrophic condition. 5. Downregulation of these two transcriptional factors might explain why CGRP suppresses the induction of many markers of autophagy and lysosome biogenesis upon muscle atrophy condition. 6. It has been shown MuRF1 plays a role in the degradation of AChR at the NMJ under atrophying conditions [5]. 7. Notably, muscle denervation process implied enhanced production of endo/lysosomal carriers of AChR, which also contained the membrane remodeler Bif1, MuRF1, and the selective autophagy receptor 62 [6]. 8. Our data are in agreement these previous studies and suggest CGRP maintains the stability of AChR at the NMJ during muscle denervation through its negative action on LC3, p62, and MuRF1. 9. Previous studies have shown calpains are involved in the degradation of AChR at NMJ [7] under atrophic conditions and PKA inhibits the fragmentation of NMJ induced by atrophic denervation [8]. Since PKA inhibits calpains [9] and because CGRP activates PKA and also inhibits calpain, our data suggest the effects of CGRP in the maintenance of NMJ might depend on the action of this peptide on calpains via PKA. 10. In summary, these results suggest CGRP maintains the stability of AChR at NMJ upon muscle atrophy induced by DEN most likely through its inhibitory action on FoxO and TFEB, a central regulator of autophagosome and lysosome biogenesis and most likely through the inhibitory action of this peptide on calpains.

the decrease in plasma levels of insulin induced by CGRP treatment *in vivo*. Indeed, CGRP is a well-known inhibitor of insulin secretion [45–47], an effect that seems to be due to the stimulation of somatostatin release [70].

In agreement with previous studies [10,13,29], our data show that the calpain system, as estimated by different approaches including the cleavage of p35 into p25, was activated in denervated skeletal muscles. Fittingly, we have observed that the calpain induction by DEN was completely abolished in skeletal muscle of rats chronically treated with CGRP. Our *in vitro* experiments also showed that CGRP inhibits the increase in the activity of Ca^{2+} -dependent proteolysis in isolated muscles and the calpain-1 autolysis in C2C12 myotubes induced by carbachol, a nonhydrolyzable cholinergic agonist that increases the cytosolic Ca^{2+} levels and activates the calpain [13]. Since CGRP also increased the amount of AChR in C2C12 myotubes incubated with carbachol and cycloheximide, CGRP controls AChR levels likely rather via the inhibition of the calpain system than by gene expression mechanisms. That calpain is implicated in the instability of the NMJ is also consistent with the present finding that the *in vivo* treatment with calpeptin, a calpain inhibitor, mimicked the effects of CGRP, and abolished the reduction of NMJ area induced by DEN. Such hypothesis is further supported by the findings that calpain participates in the dispersion and degradation of AChR clusters [13], and that it is activated at NMJs slow-channel myasthenic patients, where Ca^{2+} overload occurs at the NMJ due to mutations in the genes encoding AChR subunits [12]. Interestingly, in a mouse model of this syndrome, transgenic overexpression of calpastatin ameliorated the symptoms and neuromuscular transmission [12,13].

In summary, the present data suggest that, upon muscle denervation, the trophic effect of CGRP at NMJ is apparently mediated through a cAMP/PKA-dependent pathway, which leads to the transcriptional inhibition of FoxO/TFEB-regulated autophagic genes and stimulation of mTORC1 (Figure 8). Consequently, the degradation of AChR by autophagy-lysosome system is suppressed in the presence of CGRP. Furthermore, the inhibition of calpain system by CGRP seems to be an additional regulatory mechanism involved in the NMJ stabilization under atrophic conditions. These findings are important for identifying mediators involved in the maintenance of NMJs integrity, which may positively affect muscle function and health.

AUTHOR CONTRIBUTIONS

J. Machado and L.C. Navegantes designed the research; J. Machado performed the laboratory analyses; J. Machado, W.S. Silveira, D.A. Gonçalves, N.M. Zanon, M.M. Khan, Schavinski A.Z, Diaz M.B., and R. Rudolf performed the data collection; J. Machado, I.C. Kettelhut, and L.C. Navegantes analyzed the data; J. Machado drafted the manuscript; and all authors edited and approved the final version.

FUNDING

This work was supported by grants to Juliano Machado (FAPESP 2015/21112-7, 2011/11003-5); Wilian A. Silveira (PNPD/CAPES – PNP20131672); Dawit A. Gonçalves (FAPESP 2012/18861-0); Isis C. Kettelhut (FAPESP 2018/10089-2; 2012/24524-6; 2011/11003-5); Luiz C.C. Navegantes (FAPESP 2012/24524-6; 2011/11003-5). The

Multiphoton microscope facility is maintained by a grant from FAPESP-EMU (2009/54014-7).

ACKNOWLEDGMENTS

We thank Elza Aparecida Filippin, Lilian C. Heck, Maria Antonieta R. Garófalo, and Victor Diaz Galban for their constant technical support.

CONFLICTS OF INTEREST STATEMENT

The authors declare no potential conflicts of interest.

REFERENCES

- [1] Liu, T., Kamiyoshi, A., Sakurai, T., Ichikawa-Shindo, Y., Kawate, H., Yang, L., et al., 2017. Endogenous calcitonin gene-related peptide regulates lipid metabolism and energy homeostasis in male mice. *Endocrinology* 158(5): 1194–1206.
- [2] Stephens, T.W., Heath, W.F., Hermeling, R.N., 1991. Presence of liver CGRP/amylin receptors in only nonparenchymal cells and absence of direct regulation of rat liver glucose metabolism by CGRP/amylin. *Diabetes* 40(3):395–400.
- [3] Poyner, D.R., 1992. Calcitonin gene-related peptide: multiple actions, multiple receptors. *Pharmacology & Therapeutics* 56:23–51.
- [4] Victoria Vega, A., Avila, G., Vega, A.V., Avila, G., 2010. CGRP, a vasodilator neuropeptide that stimulates neuromuscular transmission and EC coupling. *Current Vascular Pharmacology* 8(3):394–403.
- [5] Kashihara, Y., Sakaguchi, M., Kuno, M., 1989. Axonal transport and distribution of endogenous calcitonin gene-related peptide in rat peripheral nerve. *Journal of Neuroscience: The Official Journal of the Society for Neuroscience* 9(11):3796–3802.
- [6] Sakaguchi, M., Inaishi, Y., Kashihara, Y., Kuno, M., 1991. Release of calcitonin gene-related peptide from nerve terminals in rat skeletal muscle. *The Journal of Physiology* 434:257–270.
- [7] Shen, C., Li, L., Zhao, K., Bai, L., Wang, A., Shu, X., et al., 2018. Motoneuron Wnts regulate neuromuscular junction development. *ELife* 7.
- [8] Sanes, J.R., Lichtman, J.W., 2001. Induction, assembly, maturation and maintenance of a postsynaptic apparatus. *Nature Reviews Neuroscience* 2:791–805.
- [9] Engel, A.G., Shen, X.-M., Selcen, D., Sine, S.M., 2015. Congenital myasthenic syndromes: pathogenesis, diagnosis, and treatment. *The Lancet Neurology* 14(4):420–434.
- [10] Gonçalves, D. a P., Silveira, W. a., Lira, E.C., Graça, F. a., Paula-Gomes, S., Zanon, N.M., et al., 2012. Clenbuterol suppresses proteasomal and lysosomal proteolysis and atrophy-related genes in denervated rat soleus muscles independently of Akt. *American Journal of Physiology. Endocrinology and Metabolism* 302(1):E123–E133.
- [11] Mammucari, C., Milan, G., Romanello, V., Masiero, E., Rudolf, R., Del Piccolo, P., et al., 2007. FoxO3 controls autophagy in skeletal muscle in vivo. *Cell Metabolism* 6(6):458–471.
- [12] Groshong, J.S., Spencer, M.J., Bhattacharyya, B.J., Kudryashova, E., Vohra, B.P.S., Zayas, R., et al., 2007. Calpain activation impairs neuromuscular transmission in a mouse model of the slow-channel myasthenic syndrome. *Journal of Clinical Investigation* 117(10):2903–2912.
- [13] Chen, F., Qian, L., Yang, Z.-H., Huang, Y., Ngo, S.T., Ruan, N.-J., et al., 2007. Rapsyn interaction with calpain stabilizes AChR clusters at the neuromuscular junction. *Neuron* 55(2):247–260.
- [14] Khan, M.M., Lustrino, D., Silveira, W.A., Wild, F., Straka, T., Issop, Y., et al., 2016. Sympathetic innervation controls homeostasis of neuromuscular junctions in health and disease. *Proceedings of the National Academy of Sciences of the United States of America* 113(3):746–750.
- [15] Röder, I.V., Choi, K.-R.R., Reischl, M., Petersen, Y., Diefenbacher, M.E., Zaccolo, M., et al., 2010. Myosin Va cooperates with PKA R1alpha to mediate maintenance of the endplate in vivo. *Proceedings of the National Academy of Sciences of the United States of America* 107(5):2031–2036.
- [16] New, H.V., Mudge, A.W., 1986. Calcitonin gene-related peptide regulates muscle acetylcholine receptor synthesis. *Nature* 323(6091):809–811.
- [17] Avila, G., Aguilar, C.I., Ramos-Mondragón, R., 2007. Sustained CGRP1 receptor stimulation modulates development of EC coupling by cAMP/PKA signalling pathway in mouse skeletal myotubes. *The Journal of Physiology* 584(Pt 1):47–57.
- [18] Lu, B., Fu, W.M., Greengard, P., Poo, M.M., 1993. Calcitonin gene-related peptide potentiates synaptic responses at developing neuromuscular junction. *Nature* 363(6424):76–79.
- [19] Ringer, C., Tune, S., Bertoune, M.A., Schwarzbach, H., Tsujikawa, K., Weihe, E., et al., 2017. Disruption of calcitonin gene-related peptide signaling accelerates muscle denervation and dampens cytotoxic neuroinflammation in SOD1 mutant mice. *Cellular and Molecular Life Sciences: CMLS* 74(2):339–358.
- [20] Khan, M.M., Strack, S., Wild, F., Hanashima, A., Gasch, A., Brohm, K., et al., 2014. Role of autophagy, SQSTM1, SH3GLB1, and TRIM63 in the turnover of nicotinic acetylcholine receptors (January). p. 1–14.
- [21] Wild, F., Khan, M.M., Straka, T., Rudolf, R., 2016. Progress of endocytic CHRN to autophagic degradation is regulated by RAB5-GTPase and T145 phosphorylation of SH3GLB1 at mouse neuromuscular junctions in vivo. *Autophagy* 12(12):2300–2310.
- [22] Jackman, R.W., Kandarian, S.C., 2004. The molecular basis of skeletal muscle atrophy. *American Journal of Physiology - Cell Physiology* 287(4):C834–C843.
- [23] Libby, P., Bursztajn, S., Goldberg, A.L., 1980. Degradation of the acetylcholine receptor in cultured muscle cells: selective inhibitors and the fate of ungraded receptors. *Cell* 19(2):481–491.
- [24] Rudolf, R., Bogomolovas, J., Strack, S., Choi, K.-R., Khan, M.M., Wagner, A., et al., 2013. Regulation of nicotinic acetylcholine receptor turnover by MuRF1 connects muscle activity to endo/lysosomal and atrophy pathways. *Age (Dordrecht, Netherlands)* 35(5):1663–1674.
- [25] Masiero, E., Agatea, L., Mammucari, C., Blaauw, B., Loro, E., Komatsu, M., et al., 2009. Autophagy is required to maintain muscle mass. *Cell Metabolism* 10(6):507–515.
- [26] Castets, P., Lin, S., Rion, N., Di Fulvio, S., Romanino, K., Guridi, M., et al., 2013. Sustained activation of mTORC1 in skeletal muscle inhibits constitutive and starvation-induced autophagy and causes a severe, late-onset myopathy. *Cell Metabolism* 17(5):731–744.
- [27] Tang, H., Inoki, K., Lee, M., Wright, E., Khuong, A.A., Khuong, A.A., et al., 2014. mTORC1 promotes denervation-induced muscle atrophy through a mechanism involving the activation of FoxO and E3 ubiquitin ligases. *Science Signaling* 7:ra18. February.
- [28] Penney, J., Tsurudome, K., Liao, E.H., Elazzouzi, F., Livingstone, M., Gonzalez, M., et al., 2012. TOR is required for the retrograde regulation of synaptic homeostasis at the Drosophila neuromuscular junction. *Neuron* 74(1):166–178.
- [29] Goll, D.E., Thompson, V.F., Li, H., Wei, W., Cong, J., 2003. The calpain system. *Physiological Reviews* 83:731–801.
- [30] Navegantes, L.C.C., Baviera, a M., Kettelhut, I.C., 2009. The inhibitory role of sympathetic nervous system in the Ca²⁺-dependent proteolysis of skeletal muscle. *Brazilian Journal of Medical and Biological Research* 42(1):21–28.
- [31] Hussain, H., Dudley, G.A., Johnson, P., 1987. Effects of denervation on calpain and calpastatin in hamster skeletal muscles. *Experimental Neurology* 97(3): 635–643.
- [32] Kumamoto, T., Kleese, W.C., Cong, J.Y., Goll, D.E., Pierce, P.R., Allen, R.E., 1992. Localization of the Ca²⁺-dependent proteinases and their inhibitor in normal, fasted, and denervated rat skeletal muscle. *The Anatomical Record* 232:60–77.
- [33] Karam, C., Yi, J., Xiao, Y., Dhakal, K., Zhang, L., Li, X., et al., 2017. Absence of physiological Ca²⁺ transients is an initial trigger for mitochondrial dysfunction in skeletal muscle following denervation. *Skeletal Muscle* 7(1):6.

- [34] Mammucari, C., Gherardi, G., Zamparo, I., Raffaello, A., Boncompagni, S., Chemello, F., et al., 2015. The mitochondrial calcium uniporter controls skeletal muscle trophism in vivo. *Cell Reports* 10(8):1269–1279.
- [35] Navegantes, L.C., Resano, N.M., Migliorini, R.H., Kettelhut, I.C., 2001. Catecholamines inhibit Ca(2+)-dependent proteolysis in rat skeletal muscle through beta(2)-adrenoceptors and cAMP. *American Journal of Physiology. Endocrinology and Metabolism* 281:E449–E454.
- [36] Supinski, G.S., Callahan, L.A., 2010. Calpain activation contributes to endotoxin-induced diaphragmatic dysfunction. *American Journal of Respiratory Cell and Molecular Biology* 42:80–87.
- [37] Gonçalves, D. A. P., Lira, E.C., Baviera, A.M., Cao, P., Zanon, N.M., Arany, Z., et al., 2009. Mechanisms involved in 3',5'-cyclic adenosine monophosphate-mediated inhibition of the ubiquitin-proteasome system in skeletal muscle. *Endocrinology* 150:5395–5404. December.
- [38] Machado, J., Manfredi, L.H., Silveira, W.A., Gonçalves, D.A.P., Lustrino, D., Zanon, N.M., et al., 2016. Calcitonin gene-related peptide inhibits autophagic-lysosomal proteolysis through cAMP/PKA signaling in rat skeletal muscles. *The International Journal of Biochemistry & Cell Biology* 72:40–50.
- [39] Navegantes, L.C., Resano, N.M., Migliorini, R.H., Kettelhut, I.C., 1999. Effect of guanethidine-induced adrenergic blockade on the different proteolytic systems in rat skeletal muscle. *American Journal of Physiology* 277:E883–E889.
- [40] Scharff, R., Wool, I.G., 1964. Concentration of amino acids in rat muscle and plasma. *Nature* 202:603–604.
- [41] Waalkes, T.P., Udenfriend, S., 1957. A fluorometric method for the estimation of tyrosine in plasma and tissues. *The Journal of Laboratory and Clinical Medicine* 50:733–736.
- [42] Tse, N., Morsch, M., Ghazanfari, N., Cole, L., Visvanathan, A., Leamey, C., et al., 2014. The neuromuscular junction: measuring synapse size, fragmentation and changes in synaptic protein density using confocal fluorescence microscopy. *Journal of Visualized Experiments: Journal of Visualized Experiments* 94.
- [43] Pacifici, G.M., Pellegrino, C., Maffei, C., Beconcini, D., 1981. Effect of denervation on cyclic amp regulating enzymes in the rat gastrocnemius muscle. *Italian Journal of Biochemistry* 30(1):20–29.
- [44] Suzuki, Y., Shen, T., Poyard, M., Best-Belpomme, M., Hanoune, J., Defer, N., 1998. Expression of adenylyl cyclase mRNAs in the denervated and in the developing mouse skeletal muscle. *American Journal of Physiology* 274(6):C1674–C1685.
- [45] Hermansen, K., Ahrén, B., 1990. Dual effects of calcitonin gene-related peptide on insulin secretion in the perfused dog pancreas. *Regulatory Peptides* 27(1):149–157.
- [46] Kogire, M., Ishizuka, J., Thompson, J.C., Greeley, G.H., 1991. Inhibitory action of islet amyloid polypeptide and calcitonin gene-related peptide on release of insulin from the isolated perfused rat pancreas. *Pancreas* 6(4):459–463.
- [47] Rasmussen, T.N., Bersani, M., Schmidt, P., Thim, L., Kofod, H., Jørgensen, P.N., et al., 1998. Isolation and molecular characterization of porcine calcitonin gene-related peptide (CGRP) and its endocrine effects in the porcine pancreas. *Pancreas* 16(2):195–204.
- [48] Furuno, K., Goldberg, A.L., 1986. The activation of protein degradation in muscle by Ca2 + injury does not involve a. *Lysosomal Mechanism* 864:859–864.
- [49] Gomes, a. V., Waddell, D.S., Siu, R., Stein, M., Dewey, S., Furlow, J.D., et al., 2012. Upregulation of proteasome activity in muscle RING finger 1-null mice following denervation. *The FASEB Journal* 26:2986–2999.
- [50] Wong, A.S.L., Lee, R.H.K., Cheung, A.Y., Yeung, P.K., Chung, S.K., Cheung, Z.H., et al., 2011. Cdk5-mediated phosphorylation of endophilin B1 is required for induced autophagy in models of Parkinson's disease. *Nature Cell Biology* 13:568–579.
- [51] Takahashi, Y., Coppola, D., Matsushita, N., Cualing, H.D., Sun, M., Sato, Y., et al., 2007. Bif-1 interacts with Beclin 1 through UVRAG and regulates autophagy and tumorigenesis. *Nature Cell Biology* 9(10):1142–1151.
- [52] Klionsky, D.J., Abdelmohsen, K., Abe, A., Abedin, M.J., Abeliovich, H., Arozana, A.A., et al., 2016. Guidelines for the use and interpretation of assays for monitoring autophagy (3rd edition). *Autophagy* 12(1).
- [53] Zhao, J., Brault, J.J., Schild, A., Cao, P., Sandri, M., Schiaffino, S., et al., 2007. FoxO3 coordinately activates protein degradation by the autophagic/lysosomal and proteasomal pathways in atrophying muscle cells. *Cell Metabolism* 6(6):472–483.
- [54] Sandri, M., Sandri, C., Gilbert, A., Skurk, C., Calabria, E., Picard, A., et al., 2004. Foxo transcription factors induce the atrophy-related ubiquitin ligase atrogin-1 and cause skeletal muscle atrophy. *Cell* 117(3):399–412.
- [55] Settembre, C., Zoncu, R., Medina, D.L., Vetrini, F., Erdin, S., Erdin, S., et al., 2012. A lysosome-to-nucleus signalling mechanism senses and regulates the lysosome via mTOR and TFEB. *The EMBO Journal* 31(5):1095–1108.
- [56] Du Bois, P., Pablo Tortola, C., Lodka, D., Kny, M., Schmidt, F., Song, K., et al., 2015. Angiotensin II induces skeletal muscle atrophy by activating TFEB-mediated MuRF1 expression. *Circulation Research* 117(5):424–436.
- [57] Fu, A.K.Y., Ip, F.C.F., Fu, W.-Y., Cheung, J., Wang, J.H., Yung, W.-H., et al., 2005. Aberrant motor axon projection, acetylcholine receptor clustering, and neurotransmission in cyclin-dependent kinase 5 null mice. *Proceedings of the National Academy of Sciences of the United States of America* 102(42):15224–15229.
- [58] Bodine, S.C., Latres, E., Baumhueter, S., Lai, V.K., Nunez, L., Clarke, B.A., et al., 2001. Identification of ubiquitin ligases required for skeletal muscle atrophy. *Science (New York, N.Y.)* 294:1704–1708.
- [59] Gomes, M.D., Lecker, S.H., Jagoe, R.T., Navon, A., Goldberg, A.L., 2001. Expressed during muscle atrophy. *Structure*, 1–6.
- [60] Rommel, C., Bodine, S.C., Clarke, B.A., Rossman, R., Nunez, L., Stitt, T.N., et al., 2001. Mediation of IGF-1-induced skeletal myotube hypertrophy by PI(3)K/Akt/mTOR and PI(3)K/Akt/GSK3 pathways. *Nature Cell Biology* 3:1009–1013.
- [61] Liu, D., Bordicchia, M., Zhang, C., Fang, H., Wei, W., Li, J.L., et al., 2016. Activation of mTORC1 is essential for β -adrenergic stimulation of adipose browning. *Journal of Clinical Investigation* 126(5):1704–1716.
- [62] Angliker, N., Burri, M., Zaichuk, M., Fritschy, J.-M., Rüegg, M.A., 2015. mTORC1 and mTORC2 have largely distinct functions in Purkinje cells. *European Journal of Neuroscience* 42(8):2595–2612.
- [63] Santos, V.R., Pun, R.Y.K., Arafa, S.R., LaSarge, C.L., Rowley, S., Khademi, S., et al., 2017. PTEN deletion increases hippocampal granule cell excitability in male and female mice. *Neurobiology of Disease* 108:339–351.
- [64] Mirzaa, G.M., Campbell, C.D., Solovieff, N., Goold, C., Jansen, L.A., Menon, S., et al., 2016. Association of MTOR mutations with developmental brain disorders, including megalencephaly, focal cortical dysplasia, and pigmentary mosaicism. *JAMA Neurology* 73(7):836–845.
- [65] Baldassari, S., Licchetta, L., Tinuper, P., Bisulli, F., Pippucci, T., 2016. GATOR1 complex: the common genetic actor in focal epilepsies. *Journal of Medical Genetics* 53(8):503–510.
- [66] Figlia, G., Gerber, D., Suter, U., 2017. Myelination and mTOR. *Glia* 66(4):693–707.
- [67] Zhou, J., Tan, S.-H., Nicolas, V., Bauvy, C., Yang, N.-D., Zhang, J., et al., 2013. Activation of lysosomal function in the course of autophagy via mTORC1 suppression and autophagosome-lysosome fusion. *Cell Research* 23(4):508–523.
- [68] Gonçalves, D.A., Silveira, W.A., Manfredi, L.H., Graça, F.A., Armani, A., Bertaggia, E., et al., 2019. Insulin/IGF1 signalling mediates the effects of β 2-adrenergic agonist on muscle proteostasis and growth. *Journal of Cachexia, Sarcopenia and Muscle* 10(2):455–475.
- [69] Watanabe-Asano, T., Kuma, A., Mizushima, N., 2014. Cycloheximide inhibits starvation-induced autophagy through mTORC1 activation. *Biochemical and Biophysical Research Communications* 445(2):334–339.
- [70] Demetriades, C., Doumpas, N., Teleman, A.A., 2014. Regulation of TORC1 in response to amino acid starvation via lysosomal recruitment of TSC2. *Cell* 156(4):786–799.
- [71] Menon, S., Dibble, C.C., Talbott, G., Hoxhaj, G., Valvezan, A.J., Takahashi, H., et al., 2014. Spatial control of the TSC complex integrates insulin and nutrient regulation of mTORC1 at the lysosome. *Cell* 156(4):771–785.